Behavior of Granular Pile and Granular Piled Raft

Jancy F

A Dissertation Submitted to
Indian Institute of Technology Hyderabad
In Partial Fulfillment of the Requirements for
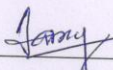The Degree of Master of Technology

भारतीय प्रौद्योगिकी संस्थान हैदराबाद
Indian Institute of Technology Hyderabad

Department of Civil Engineering

June, 2012

Declaration

I declare that this written submission represents my ideas in my own words, and where others' ideas or words have been included, I have adequately cited and referenced the original sources. I also declare that I have adhered to all principles of academic honesty and integrity and have not misrepresented or fabricated or falsified any idea/data/fact/source in my submission. I understand that any violation of the above will be a cause for disciplinary action by the Institute and can also evoke penal action from the sources that have thus not been properly cited, or from whom proper permission has not been taken when needed.
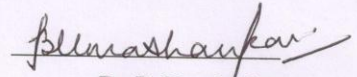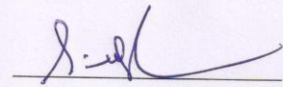
(Signature)

JANCY F
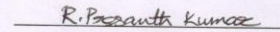(Student Name)

CE10m04
(Roll No)

Approval Sheet

This thesis entitled 'Behavior of Granular Pile and Granular Piled Raft' by Jancy F is approved for the degree of Master of Technology from IIT Hyderabad.

Dr. B. Umashankar

Assistant Professor

Department of Civil Engineering

IIT Hyderabad

Advisor

Dr. S. Sireesh

Assistant Professor

Department of Civil Engineering

IIT Hyderabad

Examiner

Dr. R. Prasanth Kumar

Assistant Professor

Department of Mechanical Engineering

IIT Hyderabad

Chairman

Acknowledgements

Dedicated to

My parents

Abstract

Granular pile, also popularly known as stone column, is an economical and efficient ground improvement technique to treat variety of soils. Depending on loading, geometry and spacing pattern, granular pile may fail individually or as a group. Bulging failure of granular pile is the most common failure criterion among the possible failure mechanisms – punching failure, shear failure and bulging failure. In this study, Finite Element analyses have been performed using commercially available software PLAXIS 2D to understand the bulging and the load-settlement behavior of both single floating granular pile and granular piled raft embedded in a soft clay deposit. Elastic-perfectly plastic response (Mohr-Coulomb criterion) is used to model both the granular pile and the soft clay. Parametric study is carried out by varying the properties of clay and granular pile to understand and quantify (a) the bulging along the depth of the pile with and without raft, and (b) the load-carrying capacity of granular pile and piled raft. Critical length of granular pile is also proposed for the cases considered in the study.

Contents

Chapter 1

Introduction

1.1 Overview

Since coastal areas are one of the most productive areas and offer good locations for trading purposes, lot of developmental activities like construction of ports, industries, tourism based buildings and other infrastructure facilities are on the rise. But as these areas mostly contain soft marine clay with very low shear strength and high compressibility, construction in these areas becomes a challenging task for Civil Engineers. The increased cost of conventional foundations restricts their applications in these areas. Ground improvement by granular piles offers a very economical and efficient remedial method. Granular piles, also known as stone columns or granular columns, are essentially made up of granular materials compacted in long cylindrical bore holes.

Even though the widespread use of granular piles is to support embankments, storage tanks, *etc*., as a group, interest in the application of granular pile as either a single granular pile or as a small group is increasing in recent times for low-rise buildings. For such instances, understanding the behavior of granular pile as a single or isolated one for reinforcing soil becomes essential. Isolated, long granular pile is usually subjected to bulging mode of failure. From the existing literature, it was found that only limited studies are available on the bulging behavior of single floating granular pile in clay deposit. Hence, in order to understand the bulging behavior, this study is carried out using finite element program PLAXIS 2D. In addition, the load-carrying capacity of single-floating granular pile and granular pile raft is quantified.

1.2 Objectives of the study

The objectives of this study are the following:

- To study bulging behavior and load-settlement behavior of single floating granular pile and granular piled raft embedded in a semi- infinite medium of clay by

1

considering linear elastic-perfectly plastic response for both granular pile and soft clay deposit.

- To carry out a parametric study to quantify the effects of various properties of clay and granular pile on bulging behavior and load-settlement behavior of granular pile and granular piled raft. The study related to bulging behavior of granular pile aims to study the effects of various properties of granular material and soft clay on the bulging depth, maximum bulging and the corresponding depth.
- To study the critical length of GP and how this affect the mode of failure of granular pile.

1.3 Organization of the study

Chapter 2 contains the theoretical background for understanding the behavior of granular pile. Chapter 3 discusses the basic ideas of numerical modeling in PLAXIS 2D to simulate elastic – perfectly plastic behavior of granular pile. Chapter 4 will give validation of numerical modeling of granular pile, non-linear analysis of granular pile, and provides the discussion on results based on bulging behavior and load-settlement behavior of granular pile. Chapter 5 discusses numerical modeling of granular piled raft, comparison of granular pile raft with granular pile, importance of evaluation of critical length of granular pile and results based on bulging behavior and load-settlement behavior of granular piled raft. Finally, Chapter 6 contains conclusions based on numerical analysis of granular pile and piled raft.

Chapter 2

Literature Review

2.1 Introduction

Currently, more than fifty percent of the World's population live in coastal areas because they are one of the most productive areas and offer good locations for trading purposes. Hence, lot of developmental activities like construction of ports, industries, tourism based buildings, and other infrastructure facilities are on the rise. But as these areas mostly contain soft marine clay with very low shear strength and high compressibility, construction on these areas becomes a challenging task for Civil Engineers. The increased cost of conventional foundations restricts their applications in these areas. Because of this, ground improvement techniques such as deep mixing method, dredging, preloading and soil displacement, *etc.*, have been widely used. But considering environmental restrictions and post construction maintenance expenses, granular piles (GP) are mostly preferred.

2.2 History and applications of granular pile

Granular pile can be defined as a compacted vertical column of stones that penetrates and replaces unsuitable soil. In 1830, the concept of stone column was first applied in France. In the early 1960s, this technique was adopted in European countries and thereafter it has been used successfully for 1) improving slope stability of both embankments and natural slopes, 2) increasing bearing capacity, 3) reducing the liquefaction potential of sands, 4) reducing total and differential settlement, and 5) increasing the time rate of settlement. Applications of stone column also include support of embankments, abutments, bridges and other type of structures. The problem of differential settlement in the case of extending an already existing embankment over soft soils may be prevented by adopting granular piles as a ground improvement technique.

Many research studies have been conducted to understand the behavior of granular pile [1, 2, 6, 28, 31, 32]. From full scale load tests on granular piles, Bergado et al. (1984) [8] and Bergado and Lam (1987) [9] proved that granular piles increased the bearing capacity by

more than 3 to 4 times that of untreated ground, reduced the settlements at least 30% and increased slope stability safety by at least 25%.

GP can be used for wide variety of soils, ranging from loose sands to soft clays and organic soils. But it is not suitable for sensitive soils because of their reduction in strength while installing granular pile. They are cost effective, utilizing low energy (environmentally responsible), technically feasible and can be constructed in the shortest period. Even though construction of granular piles is very effective method for various applications, the behavior of GP is not fully understood. Construction of GP requires careful field control and an experienced contractor.

2.3 Methods of construction of granular piles

Method of installation of GP will depend on many factors- (a) existing site condition, (b) availability of equipment, (c) availability of material in the locality, and (d) cost of installation. Based on these factors, various common methods have been adopted all over the World. These methods are briefly explained in the following sections.

2.3.1 Vibro-compaction method

This method is suitable for granular soils. In this method, vibroflot is penetrated into the ground under its weight and with help of water and vibration [7, 17]. At predetermined depth, the vibroflot is then withdrawn slowly from the ground with subsequent addition of granular back fill to construct compacted granular pile. Schematic of construction stages in vibro-compaction process is shown in Figure 2.1.

2.3.2 Vibro-replacement method

This method is used for improving fine-grained soils which have shear strength less than 40 kPa. The equipment used for this method is similar to that for vibro-compaction method. In this process, a hole is formed in the ground by inserting a vibroflot down to the desired depth with assistance of water. After making a borehole of desired depth, vibroflot is withdrawn. The uncased borehole is flushed out and filled with granular back fill in stages. Stages are shown in Figure 2.2. This method is also known as wet process since the installation of GP is done in presence of jetting water. The wet process is commonly used where borehole stability is problematic. Hence, it is mostly adopted for sites underlain by soft soils and a high ground water table.
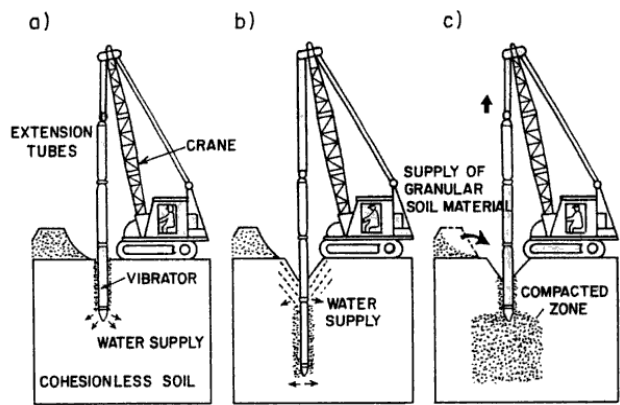
Figure 2.1: Vibro-compaction method [10]
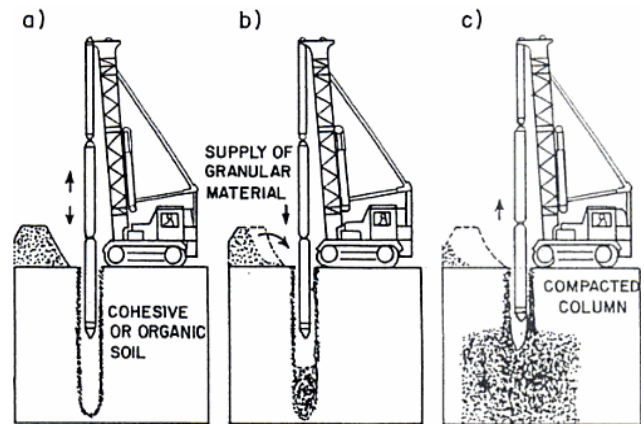
Figure 2.2: Vibro-replacement method [10]

2.3.3 Vibro-displacement method

Vibro-displacement method is also known as vibro-replacement (dry) process, since air jets are used during initial formation of borehole, instead of water jets. Construction stages for this method are same as the wet process. But, this method can only be used when the hole that is formed can withstand without collapsing during withdrawal of the probe. For suitability of dry process, soils must have undrained shear strength in the range 40-60 kN/m^2 and low ground water table condition.
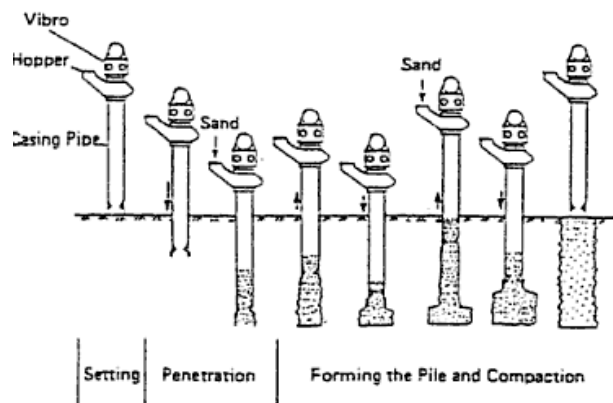
Figure 2.3: Vibro-composer method [10]

2.3.4 Vibro-composer method

The construction procedures are shown in Figure 2.3. The casing pipe is driven into the ground up to a desired depth using a heavy vertical vibratory hammer. The casing is filled with sand and then repeatedly extracted and partially re-driven using the vibratory hammer. The procedure is repeated until a fully penetrating compacted granular pile is formed. This granular pile is usually termed as sand compaction pile.

2.3.5 Cased borehole method

Granular material is rammed in stages into pre-bored holes by using a heavy falling weight of 15 to 20 kN dropped from a height of 1 m to 1.5 m. This method is more economical than vibratory compaction methods. However, its applicability might be limited to non-sensitive soils because of disturbance caused by remolding by ramming operation. Construction procedure is shown in Figure 2.4.
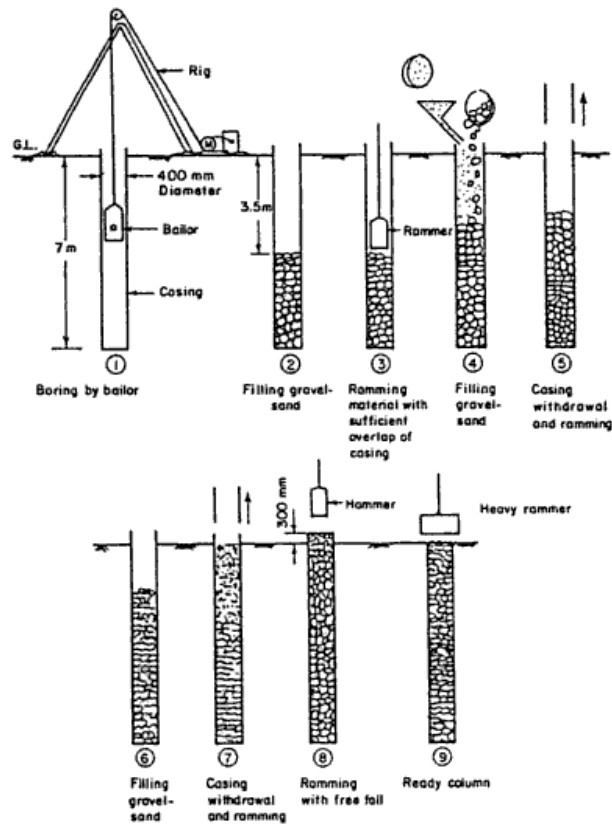
Figure 2.4: Cased-borehole process [10]

2.4 Failure mechanisms

In practice, granular piles are constructed as end bearing or floating piles. GP may fail individually or as a group. The possible failure mechanisms of single granular pile include bulging failure, shear failure, and punching failure as shown in Figure 2.5 [6]. Short granular pile may undergo either general or local bearing type failure.
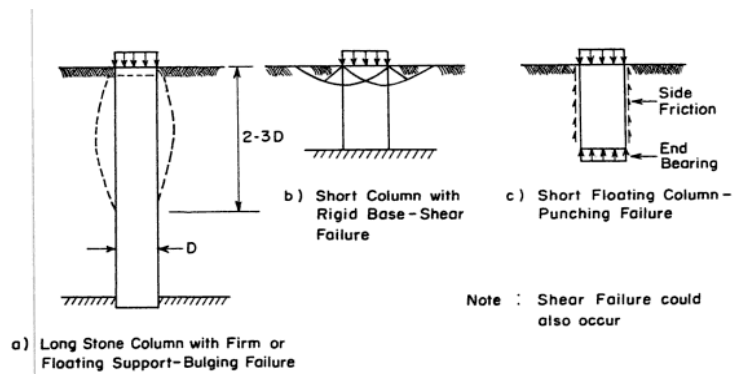
Figure 2.5: Failure mechanisms of single granular pile [6]

But in granular pile groups, since surrounding soil provides additional support to the interior piles, they are more confined leading to increased stiffness of group. Hence, they undergo

7

less bulging compared to single isolated GPs. Groups can also fail by lateral spreading especially for a wide flexible loading (embankment). The lateral spreading slightly promote the tendency of bulging of GPs. Group of piles in soft soil probably undergo a combined bulging and local bearing type failure as shown in Figure 2.6. GP groups of short length can either fail in end bearing or bearing capacity type failure of individual pile [6].
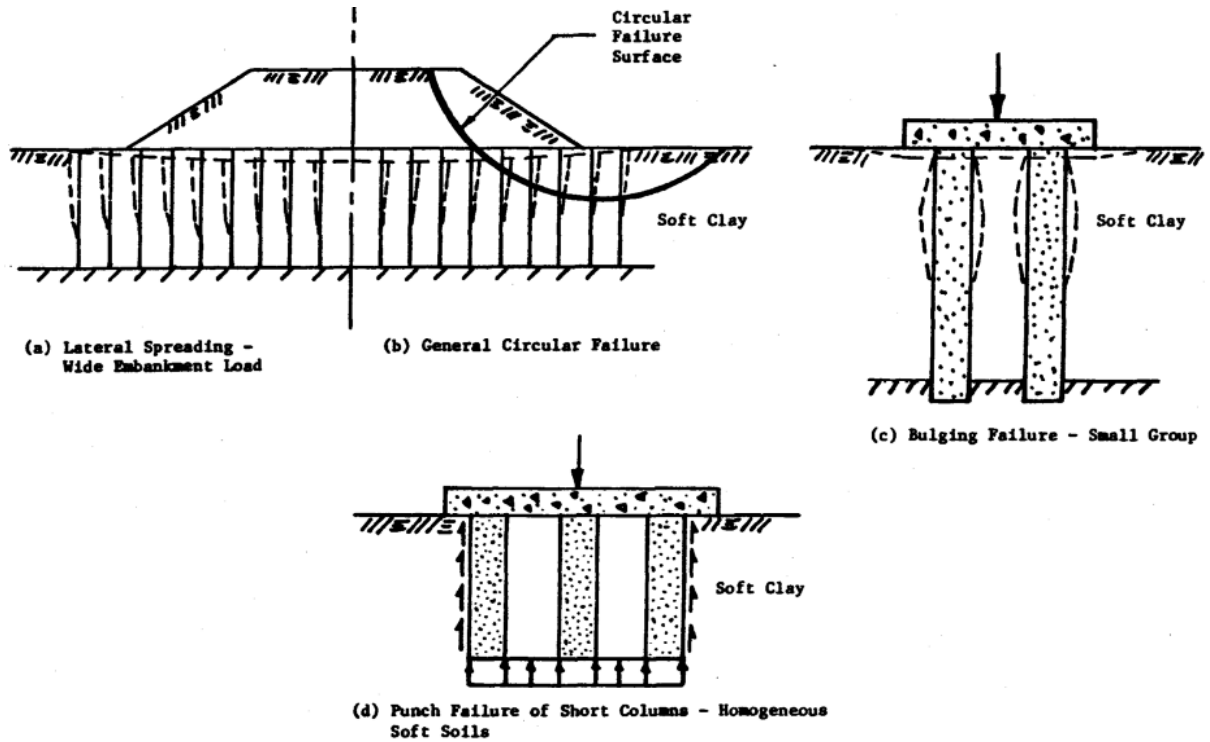
Figure 2.6: Failure mechanisms of granular pile group [6]

In this study, we focus on the bulging behavior of single isolated floating granular pile. To understand the bulging behavior of GPs, many studies based on numerical modeling, laboratory testing and field testing have been carried out. If the length of granular pile is greater than 4 to 6 times its diameter, the failure mechanism shall be the bulging mode irrespective of whether it is end bearing- or floating- type pile [23]. The bulging failure is the most common failure criterion, since most of constructed GPs in the field have length which is equal to or greater than 4 to 6 times its diameter [15]. The lateral confining stress support from the surrounding soil will affect the overall performance of the pile. Since the lateral support from the soil increases with depth, bulging mostly occurs near to the top of the pile except for cases such as the presence of intermediate layer of very weak soil like peat with thickness greater than about one pile diameter [6]. According to the studies by Barkdale and Bachus (1983) [6] and Nayak et al. (2011) [26], bulging depth will be equal to 2 to 3 times the pile diameter. Nayak et al. (2011) [26] found that the maximum bulging

occurs at a depth of 0.5 to 0.8 times the diameter of pile from the surface. Ambily and Gandhi (2007) [3] reported that the maximum bulging occurs at a depth of 0.5 times diameter of the granular pile, if GP is loaded alone. These studies consider the group effects of GPs using unit cell concept. But, Deb et al. (2011) [15] observed that the maximum bulging occurs at a depth of 1.2 times of column diameter in the case of the granular pile used to improve clay deposit and bulging diameter is equal to 1.24 times the pile diameter. In this study, groupeffect is not considered. Since these observations in this study based on small scale model tests, these have limitations of scale and boundary effects. Some field tests are reported in the literature on the bulging behavior of GPs [8, 9, 21, 22]. These field tests are reviewed in the Chapter 3.

2.5 Methods to predict the ultimate load carrying capacity of granular pile

As we have discussed, bulging failure is the most probable failure mechanism of isolated single granular pile. A number of theories have been developed for estimating the ultimate load carrying capacity of single granular pile. The lateral confining stress which is mobilized by surrounding soil, as the GP material undergoes lateral, outward displacement, is taken as the ultimate passive resistance (σ_3). This lateral passive resistance acts in the horizontal direction and triaxial state of stress is assumed within the pile. Most of these theories were developed based on this concept. According to plasticity theory, ultimate vertical stress (σ_1) can be calculated using the following equation:

$$\sigma_1 = \sigma_3 K_p \tag{2.1}$$

where, K_p (coefficient of lateral passive earth pressure) = $(1+\sin \varphi_p)/(1-\sin \varphi_p)$

φ_p = angle of shearing resistance of granular pile

Similar concept was used by Greenwood (1970) [20] for his preliminary analyses of granular piles. According to him, ultimate lateral stress can be calculated using the following equation:

$$\sigma_3 = \gamma_c z k_{pc} + 2c_u \sqrt{k_{pc}} \tag{2.2}$$

where, γ_c = unit weight of clay

z = depth of maximum bulging

k_{pc} = passive earth pressure coefficient of clay

c_u = undrained shear strength

Using Equations (2.1) and (2.2), ultimate vertical stress can be found out. But in this approach, the lateral resistance by the surrounding soil was taken as passive resistance

behind a long retaining wall. As plane- strain loading condition is assumed for modeling of granular pile, this approach does not represent actual three- dimensional geometry of a granular pile.

Using cavity expansion theory, lateral expansion of pile can be better idealized as a cylindrical expansion into the soil. This theory assumes granular pile as infinitely long cylinder which expands about the axis of symmetry. Even though the granular pile bulges radially to a distance of about 2 to 3 pile diameters, this approximation of an infinitely long expanding cylinder gives reasonable good results [21]. If the soil is treated as ideal elasto-plastic material, ultimate lateral stress (σ_3) of the granular pile was given by Gibson and Anderson (1961) [19] as

$$\sigma_3 = \sigma_{ro} + c_u[1 + \ln(E_s/2c_u(1+\mu))] \tag{2.3}$$

Where σ_{ro} = total in-situ lateral stress

     E_s = Deformation modulus of the soil

     c_u = undrained cohesion

     μ = Poisson's ratio

Hughes and Withers (1974) [21] presented a method which is based on cavity expansion theory given by Gibson and Anderson (1961) [19] for a frictionless soil. They considered the bulging or lateral expansion of granular piles as similar to the cavity developed during quick pressuremeter test. From the results of quick pressuremeter tests, they reasonably approximated the expression for the ultimate lateral stress as

$$\sigma_3 \approx \sigma_{ro} + 4c_u \tag{2.4}$$

The ultimate vertical stress of the granular pile is then calculated as

$$\sigma_1 = (\sigma_{ro} + 4c_u) \ (1+\sin \varphi_p)/ \ (1-\sin \varphi_p) \tag{2.5}$$

To incorporate for soils with both friction and cohesion, Vesic (1972) [29] had developed a general cylindrical cavity expansion solution from previous work. In his approach, soil is again assumed as elastic or plastic and pile is idealized as infinitely long cylinder. According to Vesic cavity expansion theory, the ultimate lateral passive resistance (σ_3) can be represented as

$$\sigma_3 = cF_c + qF_q \tag{2.6}$$

where, c = cohesion of the soil

     q = mean isotropic stress $(\sigma_1 + \sigma_2 + \sigma_3)/3$ at equivalent depth

     F_c, F_q= Cavity expansion factors.

Using Equations 2.1 and 2.6, ultimate vertical stress (σ_1) can be estimated. For frictionless soil, Vesic cavity expansion theory will give same result as that from cavity expansion theory given by Gibson and Anderson. Bulging failure can be estimated by these theories.

Radial expansion of granular pile can be reduced by increasing the confining stress developed within the surrounding soil. To increase the lateral confining stress, techniques such as wrapping the individual granular piles with geosynthetics [25] or with geogrids [17] or providing rigid raft on the top of granular piles [24] have been proposed. Encasement by geosynthetics or geogrid imparts additional confinement to the granular pile, thus reducing the bulging of granular pile [17, 24]. Application of load through a rigid raft over an area greater than the granular pile increases the vertical and lateral stress in the surrounding soft soil. The larger bearing area together with additional confinement of the granular pile reduces the bulging and increases the ultimate load carrying capacity. The available literature considers linear stress-strain response of soil and granular pile to model the behavior of raft foundation supported on granular pile. However, linear stress-strain response can only be applied for strains within elastic regime. In this study, elastic-perfectly plastic response of soil and GP was considered to model the behavior of single/isolated floating granular pile with and without raft. Numerical modeling was done using commercially available finite element software - PLAXIS 2D version 9.

Chapter

Numerical Modeling

3.1   Introduction

Application of advanced numerical modeling methods helps to improve the reliability on engineering design and provide economically optimized design. Numerical modeling mainly involves use of finite element or finite difference methods to analyse the problem with the help of computer. Among the available methods, finite element analysis (FEA) or finite element method (FEM) is the most popular one. The basic idea of finite element method is to divide the structure or region into large number of finite elements which are interconnected by nodes, analyse each element in local co-ordinate system and combine the results in global co-ordinate system to get the unknown variable for the entire system. This method is a suitable alternative to overcome the disadvantage of closed-form analytical solutions. In FEM, complex region is discretised into finite elements and analysed to find out the unknown field variables with the help of interpolating polynomials. This procedure can be applied to all problems which may be structural or non-structural. This speciality made FEM as one of the most powerful methods in various fields. In numerical modeling of geotechnical engineering problems, soil is usually modeled as a continuum with an appropriate constitutive model and boundary conditions. The constitutive model describes how the material behaves under specific loading conditions. The boundary conditions define the loading and displacements at the boundaries. In this study, commercially available finite element software program- PLAXIS 2D (2009) - is used. A brief description of this software is given in the following section.

3.2   PLAXIS 2D- Finite element program

3.2.1 Model

In PLAXIS 2D [13], two dimensional finite element analyses can be performed either with plane strain or axisymmetric conditions. Plane strain model is used for geometry with uniform cross section which have large dimension of geometry in one direction compared to other directions. Deformation or strain perpendicular to cross section is assumed as negligible compared to cross sectional strains or deformations. Axisymmetric model is used for uniform circular geometry with loads applied symmetrically around the central axis. In both plane strain and axisymmetric cases, each node can undergo two translations (degrees of freedom) along x –axis and y-axis. In this study, axisymmetric model is used since GP and raft have uniform circular shape.

3.2.2 Element type

The user can select 6-node or 15-node triangular elements to model region and structures in PLAXIS 2D (Figure 3.1). The 15-noded element has fourth order interpolation for displacements and twelve Gauss points or stress points for the numerical integration, whereas 6-noded element uses second order interpolation and three Gauss points. The 15-noded element is preferred over 6-noded element because of its very accurate and high quality stress results. Even though the 6-noded triangular element gives good results, it over predicts the bearing capacity and safety values for axisymmetric problems. However, use of 15-node elements leads to high memory consumption, slow calculation and slow operational performance compared to 6- node elements. For the present analysis, 15-node elements are used.
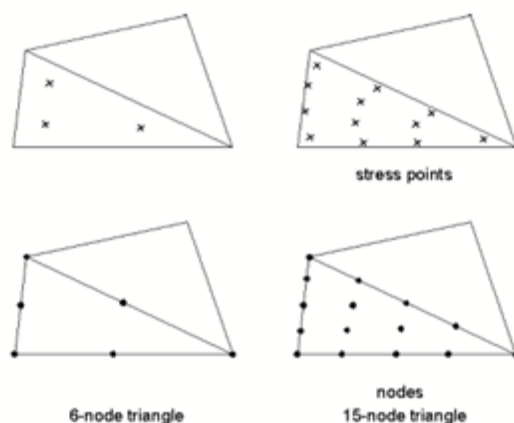

Figure 3.1: Available element types in PLAXIS 2D [13]

3.2.3 Interface elements

Interface elements enable to study the interaction between structural objects (walls, plates, geogrids, *etc.*) and surrounding soil. In modeling, corners in stiff structures and an abrupt change in boundary conditions may lead to non-physical stress oscillations. This problem can be solved by using interface elements.

Failure of long GP is due to radial bulging occurring near its top for both floating and end bearing, but not by shear failure. Hence, interface elements are not adopted in this study. In addition, depending on the installation method of GP, shear strength of the interface between GP and soft clay which is a mixed zone of stones and clay, is varying. Since this is not known precisely, use of interface elements is insignificant [3].

3.2.4 Meshing

After defining the geometry model and assigning material properties to the model, the geometry has to be divided into finite elements for analyzing of the problem. A composition of interconnected elements is called a mesh. In PLAXIS, the generation of the mesh is done by using unstructured 15-noded or 6-noded triangular elements. The sizes of mesh in the software are generally divided into five levels of global coarseness. They are very coarse, coarse, medium, fine and very fine. By default, the global coarseness is set to 'Coarse'.

3.2.5 Loads and boundary conditions

PLAXIS have options for introducing load either at the model boundaries or inside the model. Load options contain distributed load, line loads, point loads and prescribed displacement. Prescribed displacements are special conditions that can be forced on the model to control the displacements of certain points. The distributed load in the geometry model can be created similar to creating geometry line. The distributed load will be a unit pressure perpendicular to the boundary. The point load is applied in terms of force per unit width. For axisymmetric loads, point loads are actually line loads on a circle section of 1 radian. The actual point load must be divided by 2π to get the input value of the point load to be applied at the centre of the axisymmetric model [13].

Boundary conditions can be applied using fixity option. Fixities are defined as prescribed displacements at geometry line which is equal to zero. Fixity can be provided by using either horizontal ($u_x=0$), vertical ($u_y=0$), total fixity ($u_x=u_y=0$) or standard fixity. By selecting standard fixity, PLAXIS automatically imposes a set of general boundary conditions to the geometry model. These boundary conditions are generated according to the following rules [13].

- Vertical geometry lines for which the x-coordinate is equal to the lowest or highest x-coordinate in the model obtain a horizontal fixity ($u_x=0$).

- Horizontal geometry lines for which the y-coordinate is equal to the lowest y-coordinate in the model obtain a full fixity ($u_x=u_y=0$).
- Plates that extend to the boundary of the geometry model obtain a fixed rotation in the point at the boundary ($\Phi_z=0$) if at least one of the displacement directions of that point is fixed.

Since standard fixity is convenient and fast input option, it is better option for this study.

3.2.6 Modeling soil behavior

In PLAXIS, various soil models are available to simulate the behavior of soil and other structural elements. They are Linear Elastic model, Mohr-Coulomb model, Jointed Rock model, Hardening Soil model, Soft Soil model, Modified Cam-clay model, Soft Soil Creep model and User-Defined model. Among all the models, Mohr-Coulomb model will serve as a first-order approximation of real soil behavior. This elastic-perfectly plastic model requires five basic soil input parameters, namely deformation modulus (E), Poisson's ratio (μ), cohesion (c), friction angle (φ) and dilatancy angle (ψ). The failure envelope of this elastic- perfectly plastic model is shown in Figure 3.2.
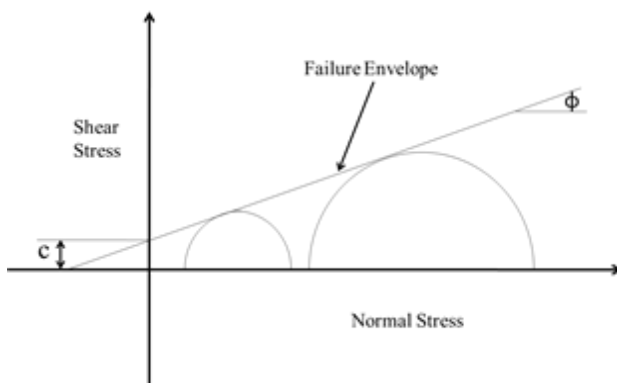
Figure 3.2: Mohr-Coulomb failure criterion

This model which is based on the combination and generalization of Hooke's and Coulomb's law, formulated in a plasticity framework. The general state of stress, failure criterion and flow rules are represented by E and μ, φ and c, and ψ respectively. According to the Mohr- Coulomb failure criterion, the failure of soil will occur when shear stress on any soil element reaches the critical value. The representation of Mohr-Coulomb failure criterion in terms of Principal stresses σ_1, σ_2 and σ_3 is shown in Figure 3.3.

In general, all model parameters are meant to simulate the effective soil state. The presence of pore water will influence significantly the behavior of soil. To incorporate the pore pressure effect, three types of behavior are available in the software: *drained* behavior, *undrained* behavior and *non-porous* behavior. Drained behavior is used for representing the

cases of no excess pressure such as dry soils, high permeable soils and/or low rate of loading. This type is mainly meant to simulate long-term soil conditions.

Figure 3.3: Mohr- Coulomb failure surfaces in principal stress space

Undrained behavior is used for simulating the excess pore pressure in cases of low permeability soils, and/or high rate of load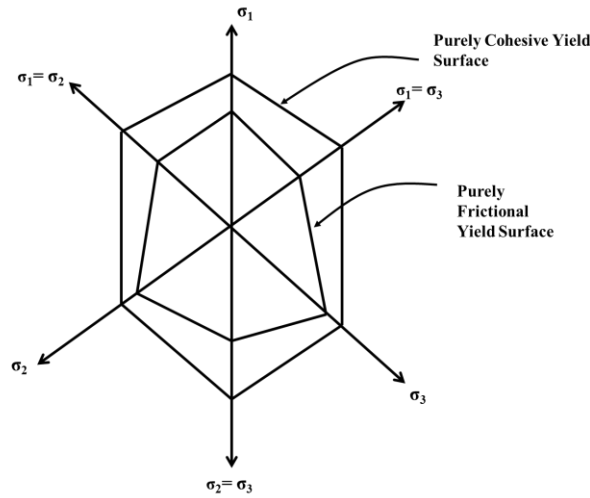ing. Undrained analysis can be done with effective stress parameters or with total stress parameters. If the effective stress parameters are known, it is possible to specify undrained behavior using effective parameters. However, if accurate effective parameters are not available, it is possible to perform a total stress analysis using stiffness parameters (undrained deformation modulus E_u and an undrained Poisson's ratio μ_u) and strength parameters (undrained shear strength c_u and $\varphi_u=0$).

For cases where initial or excess pore pressure is not to be considered, such as in the modeling concrete or structural elements, non-porous behavior is used for simulating actual behavior of these materials.

3.3 Mohr-Coulomb Model

Mohr-Coulomb model is a simple model which is highly recommended when soil parameters are not known with great certainty. This model is also applicable to three dimensional stress space modeling. Even though it simulates drained condition in a good manner, the effective stress path may deviate significantly from observed behavior in the case of undrained condition. Hence, it is preferable to use the undrained shear strength parameters in an undrained analysis with zero friction angle. This model is not suitable for tunnel and excavation problems. As already mentioned, Mohr-Coulomb model requires five basic soil input parameters, namely deformation modulus (E) or shear modulus (G), Poisson's ratio (μ), cohesion (c), friction angle (φ) and dilatancy angle (ψ). These parameters are briefly explained in the following section.

3.3.1 Deformation modulus

It may be estimated from empirical equations, laboratory test results on undisturbed specimens or from in situ tests. Laboratory tests that are used for estimating the modulus include triaxial unconsolidated undrained compression or triaxial consolidated undrained compression tests. Field tests include the plate load test, cone penetration test, standard penetration test (SPT) and pressuremeter test. The undrained deformation modulus E_u of cohesive soil can be empirically related to undrained shear strength as [16, 27].

$$E_u = Kc_u \tag{3.1}$$

Values of K range from 100 for very soft soils to as high as 1000 for very stiff clays. In this study, since soft clay is considered for this study, range of K is taken from 100 to 200.

Instead of inputting deformation modulus (E), shear modulus (G) or constrained modulus (E_{oed}) can be used. Software automatically re-calculates the deformation modulus using following equations:

$$G = E/2(1+\mu) \tag{3.2}$$

$$E_{oed}= (1-\mu)E/(1-2\mu)(1+\mu) \tag{3.3}$$

3.3.2 Poisson's ratio

Selection of Poisson's ratio, defined as ratio of longitudinal strain to lateral strain, is simple when the elastic model or Mohr-Coulomb model is used for gravity loading. For this type of loading, PLAXIS should give realistic value of coefficient of earth pressure at rest ($K_0=\sigma_h/\sigma_v$). As both the models provide a well-known ratio for one dimensional compression, it is easy to select a proper value which gives a realistic value of K_0. In most of the cases, the value of Poisson's ratio is the range of 0.3 to 0.4. For unloading situations, a lower value of Poisson's ratio (nearly 0.2) is commonly more suitable. For undrained behavior, an effective value of Poisson's ratio is highly recommended if *Undrained* behavior is selected for material behavior. PLAXIS will automatically add bulk stiffness for pore water based on implicit undrained Poisson's ratio of 0.495. In this case, the effective Poisson's ratio should be smaller than 0.35.

3.3.3 Cohesion (c)

PLAXIS can handle both cohesionless soils and cohesive soils. In the Mohr-Coulomb model, *drained* and *undrained* type of behavior, the cohesion parameter may be used to model the effective cohesion $c^{'}$ of the soil, in combination with a realistic effective friction angle φ'. PLAXIS performs an effective stress analysis for both cases. For cohesionless soil ($c^{'} \approx 0$), some options will not be performed well, especially when the corresponding soil layer reaches the ground surface. To avoid numerical issues, it is advised to enter a small value (c of the order of 0.2 kPa).

3.3.4 Friction angle

To perform an effective stress analysis of soil, the effective friction of the soil is used with an effective cohesion c'. Total stress analysis can be performed by setting the cohesion parameter equal to the undrained shear strength of the soil, in combination with $\varphi = 0$.

3.3.5 Dilatancy angle (ψ)

The dilatancy angle in case of heavily over consolidated clays and normally consolidated clays tends to zero. The dilatancy of sand depends on both the density and on the confining stress. The order of magnitude for dilatancy angle may be taken as $\varphi\text{-}30^{o}$. In most of the cases, the dilatancy angle is zero for soils which have values of friction angle less than 30° [13]. A small negative value of ψ is realistic for the case of very loose sand. In the case of associated flow rule, friction angle is equal to dilatancy angle, whereas for non-associated flow rule, dilatancy angle is not equal to friction angle.

Chapter 4

Analysis of Single Floating Granular Pile

4.1 Introduction

Granular piles are usually provided as a group to support various geotechnical structures, for example, embankments, storage tanks, *etc*. Many studies, both experimental and numerical, have been carried out to study the behavior of granular pile in a group [3, 4, 5, 11, 15, 28, 32]. For relatively moderate loading from a structure, interest in the application of granular pile either singly or in a small group is increasing in recent times. In this chapter, finite element program PLAXIS 2D, which is described in chapter 3, is used to perform non-linear analysis of isolated granular pile embedded in a semi-infinite medium of clay. The objective of this study is to determine the parameters significantly affecting the load-settlement and bulging behavior of GP. In addition, ultimate load capacity of granular pile is estimated and compared with various available theories.

4.2 Problem Definition

The objective of this Chapter is to study the load-settlement and bulging behavior of a single floating granular pile in semi- infinite medium of clay (Figure 4.1). Mohr-Coulomb's criterion is used to model linear elastic -perfectly response of clay and GP. For analysis, the finite element program PLAXIS V9 is used. The granular pile and clay is modeled as axi-symmetric 2D problem.
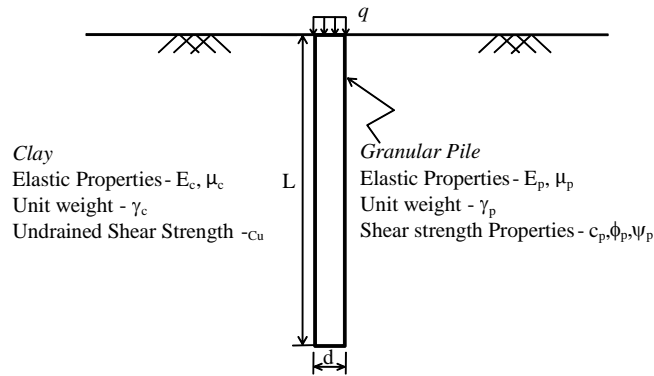
Figure 4.1: Schematic of granular pile in semi-infinite medium of clay

4.3 Validation of the model

In modeling the problem, the element size of mesh and the extent of the lateral and bottom boundaries should be properly chosen to obtain realistic values. Hence, as a first step, validation of the model was carried out with the models available in the literature. The present model was validated against the following cases from the literature:

1) Madhav et al.'s study (Linear analysis of granular pile)
2) Ambily and Gandhi's study (Non-linear analysis of granular pile in a group)
3) Hughes et al.'s study (Field tests on granular pile)

4.3.1 Validation with Madhav et al.

In this model, linear stress-strain behavior is considered for both soil and GP. It is modelled as axisymmetric case in software PLAXIS V9. The granular pile of length 10 m and diameter 1 m is considered. The soil is modelled as single layer of clay as shown in Figure 4.2. To study the effect of boundary, distance of boundaries both in lateral and vertical directions are varied and the analysis is performed. Along the bottom boundary, lateral and vertical deformations are restrained (u_x and u_y = 0). Along the lateral boundaries, lateral deformation is restrained but vertical deformation is allowed (u_x =0). A prescribed placement of 13 mm is applied on the top of GP. The elastic parameters- Deformation modulus (E) and Poisson's ratio (μ) - used in the model are given in Table 4.1.
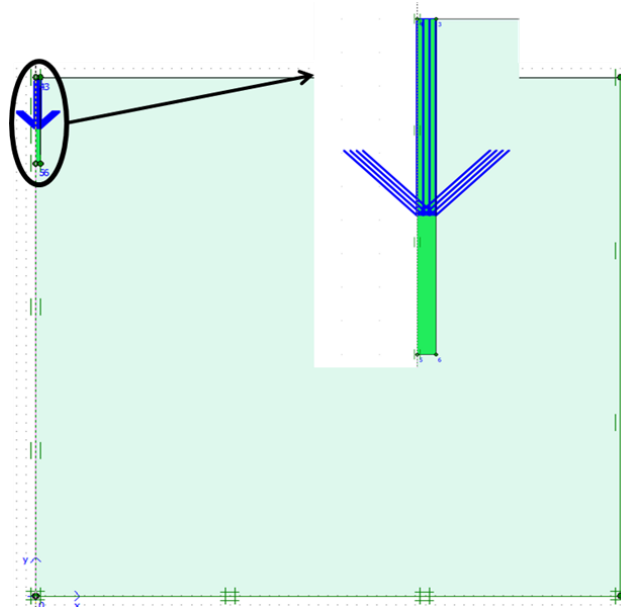
Figure 4.2: Model of granular pile and soil with the insert showing the enlarged view near the pile top

To study the effect of mesh size, analyses are performed for coarse, medium, fine and very fine mesh. Table 4.2 shows information on the generated meshes. For this study, depth and width of soil medium are taken as 60 m. 15- noded element, which is more accurate than 6-noded elements, is used for modelling this problem.

Table 4.1: Material properties of GP and soil

Properties	Soil (clay)	Granular Pile
E (Deformation Modulus) kN/m^2	3000	30000
μ (Poisson's ratio)	0.5	0.3

For each type of mesh, load corresponding to 13 mm prescribed displacement is calculated at the centre of granular pile. It is observed that load taken by GP converges as the mesh configuration is varied from coarse mesh to very fine mesh. Then, further refinement is done within and near the GP geometry. Medium mesh with further refinement and very fine mesh with further refinement give same results. Hence, medium mesh is used for entire domain and further refinement is done within and near the GP. Soil is considered as semi-infinite medium. To model soil, different values of depth and width are taken and analysed. From the analysis, we can observe that beyond a value equal to 60 m of depth of bottom

boundary and left/right lateral boundary, there is no change in value of load taken by GP. Hence, size of bottom boundary and lateral boundary is fixed as 60 m.

Very fine mesh is used for modelling.

Table 4.2: Details of generated meshes

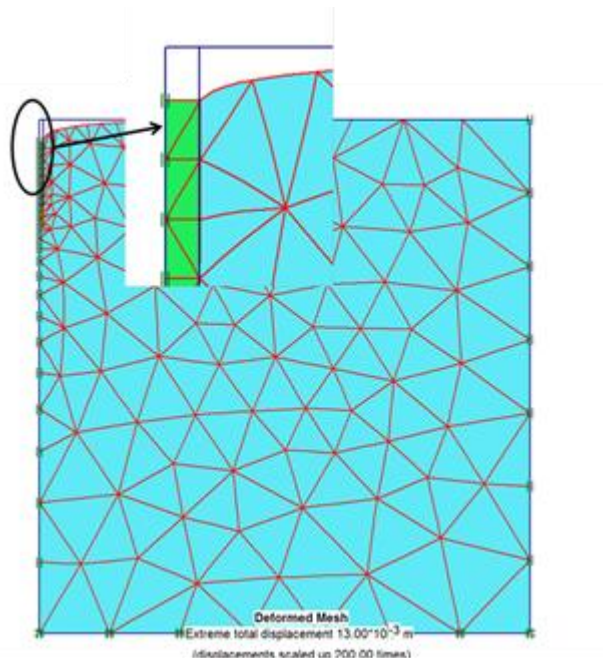| Mesh	No of elements	No of nodes	Av. Element size
Very fine	1222	9957	1.14 m
Fine	595	4891	1.64 m
Medium	276	2301	2.41 m
Coarse	128	1089	3.54 m

Figure 4.3: Deformed mesh of the model with the insert showing the enlarged view of GP

The deformed mesh of granular piled raft and soil is shown in Figure 4.3. Different values of modular ratio K (ratio of deformation modulus of granular pile to that of clay) are considered for the analysis. The load corresponding to 13 mm prescribed displacement on the top of GP is compared with solution by Madhav et al. (2009) [24]. The results from the present study show good agreement with Madhav et al. (2009) as shown in Figure 4.4.
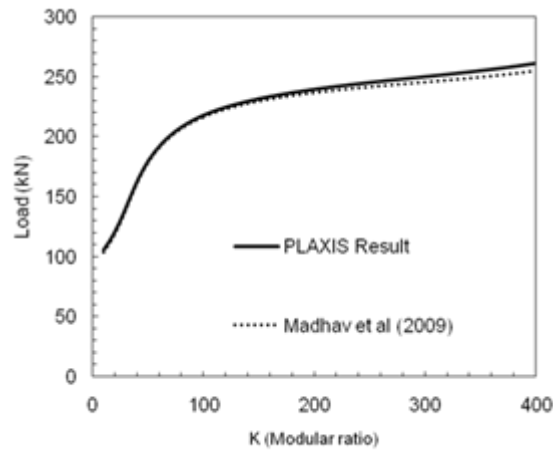
Figure 4.4: Effect of modular ratio on load taken by granular pile

4.3.2 Validation with Ambily and Gandhi

In this analysis, soft clay and granular pile is modelled using Mohr-Coulomb criterion (linear elastic-perfectly plastic). To start with, the model developed in PLAXIS 2D considering elastic-plastic response is compared with a similar study conducted by Ambily and Gandhi (2007) [3].

Model developed by Ambily and Gandhi (2007) studies the behavior of interior columns among a large group of columns. Here, interior column was idealized as unit cell as shown in Figure 4.5. They considered the following cases.

1) Granular pile loaded alone

2) Granular pile and surrounding soil loaded (sand pad is provided on the top)

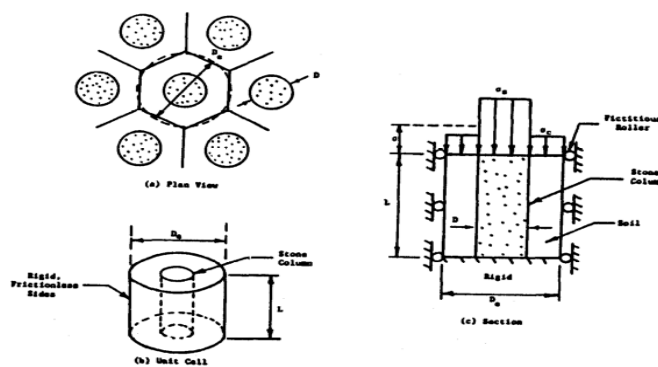**Figure 4.5: Unit cell idealization [6]**

Granular piled raft considered in Ambily and Gandhi (2007) was taken as axisymmetric case. The input parameters used in PLAXIS analysis are given in Table 4.3. The drained behaviour is considered for clay, stone column, and sand. The simulation of unit cell model is initialized by applying initial stresses in all materials using K_0 procedure. To get equal

vertical strain condition, load is applied as prescribed displacement. Water influence is not taken into account. Fine meshes which are generated using 15-noded triangular elements and boundary conditions for both the cases are shown in Figure 4.6. Along the lateral boundaries, radial deformation is restricted but vertical deformation is allowed. Along the bottom boundary, radial and vertical deformations are restricted. In this analysis, no interface element is used.

Table 4.3: Details of material properties

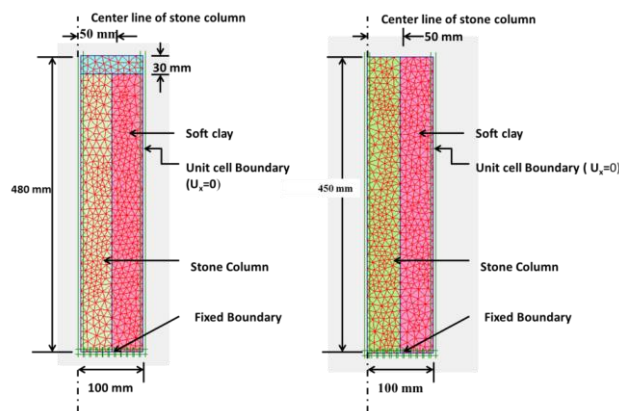| Materials	Deformation Modulus E (kN/m^2)	Poisson's ratio μ	Cohesion c_u (kN/m^2)	Dilatancy Ψ (Degree)	Friction angle φ (Degree)	Dry density (kN/m^3)	Bulk density (kN/m^3)
Soft Clay	5,500	0.42	30	_	_	15.56	19.45
Stones	55,000	0.3	_	10°	43°	16.62	_
Sand	20,000	0.3	_	4°	30°	15.50	_

Figure 4.6: Finite-element discretization for both cases

Figure 4.7 shows deformed mesh at failure for both cases. In the case of column alone loaded, bulging failure occurs with maximum bulging at a depth of 0.5 times diameter of granular pile as was noticed in Ambily and Gandhi's study [3]. For the case of entire area loaded, no bulging is observed and similar behavior reported in their analysis.
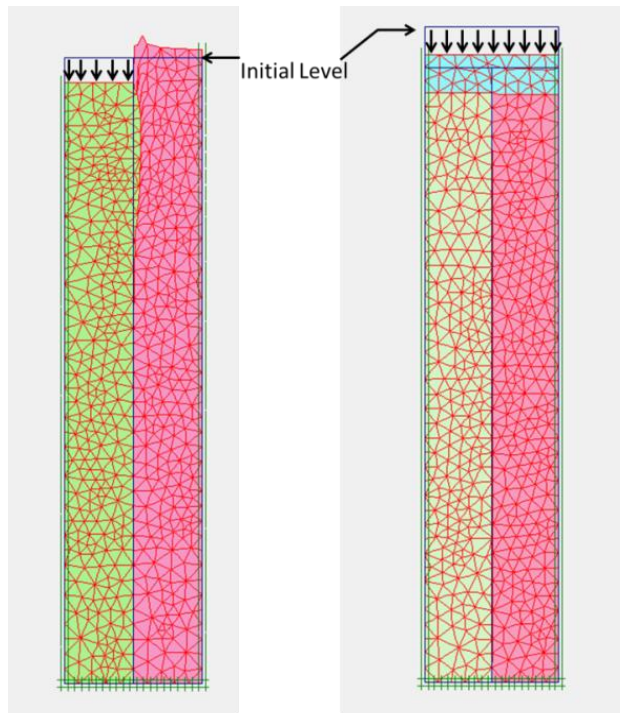
24

Figure 4.7: Deformed mesh for both cases

Based on the axial stress developed at the pile top and settlement behaviour, for the case of granular pile loaded alone, it can be observed that GP reaches a failure stage. Settlement behavior of granular pile with respect to axial stress is shown in Figure 4.8. But for second case, failure did not take place even for a large settlement of 35 mm and it is in linear elastic range of loading. Figure 4.9 shows axial stress versus settlement behavior from experimental and numerical analysis reported by Ambily and Gandhi (2007) and PLAXIS analysis. The results from the present analysis match well with Ambily and Gandhi (2007).
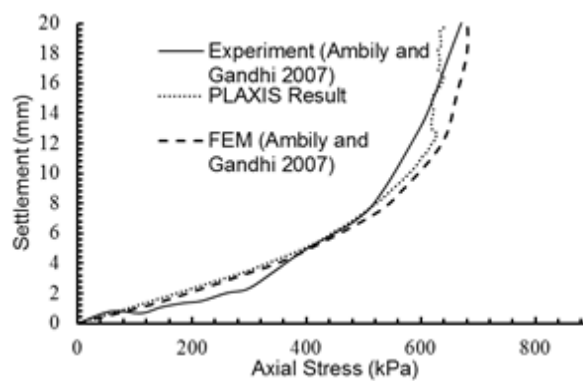

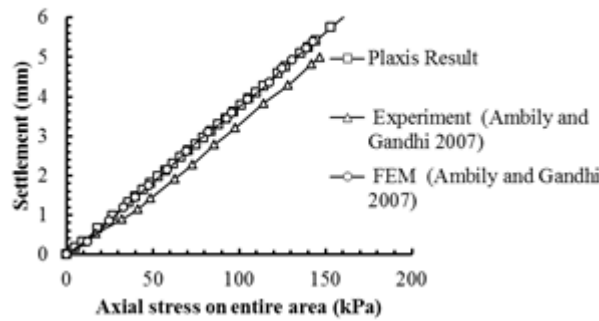**Figure 4.8: Axial stress *vs*. settlement- Granular pile alone loaded**

Figure 4.9: Axial stress *vs*. settlement- Entire area loaded

4.3.3 Validation with Hughes et al.

Full scale load test on compacted granular piles on soft Bangkok clay was done by Bergado et al. (1984) [8] to determine the ultimate load capacity of pile. Nine granular piles were constructed in a triangular pattern at a spacing of 0.9 m. Out of nine piles; seven piles were made of sand. Other two were constructed as isolated piles, one was made of sand and other was made of gravel. All piles have 0.3 m diameter and 8 m length which were penetrated into the soft Bangkok clay. The piles were compacted in lifts of 0.6m with 15 blows. From this full scale load tests, it was observed that the ultimate load capacity were 3 to 4 times greater than the untreated soil layer. It was also found that granular pile will act independently if the spacing of piles is equal to or greater than 3 times the pile diameter.

Bergado and Lam (1987) [9] investigated the behavior of the granular piles constructed with different proportions of gravel and sand compacted at different number of blows per layer under full scale load tests. Totally thirteen granular piles were installed at 1.2 m spacing in a triangular pattern. All piles which were constructed by using cased bore hole method have diameters of 0.3 m and lengths of 8 m. The piles were grouped into 5 categories. Groups 1, 2 and 3 were constructed with sand compacted at 20, 15, and 10 blows per layer, respectively. These groups consisted of 3 piles each. Group 4, consisting of two piles, was constructed using gravel mixed with sand in the proportion of 1: 0.3 by volume, and Group 5, made up of with two piles, was made of gravel. These two groups were compacted at 15 blows per layer. Four active piezometers and two dummy piezometers were installed to monitor pore water pressures. In-situ vane tests and pressuremeter tests were used for finding the soil properties. The full scale plate load tests were used for determining ultimate load capacity of piles. From this study, it was found out that the ultimate bearing capacity is directly proportional to the number of blows per layer. It was observed that gravel was the most efficient granular pile material, even though compacted at lower number of blows per

layer, due to its higher angle of shearing resistance. It was also observed that maximum bulging occurred at a depth between 10 cm to 30 cm below the ground surface.

Hughes et al. (1975) [22] had investigated the load-settlement relationship of an isolated granular pile based on field full scale plate load test. The pile was constructed in soft clay at Canvey island, Britain, using vibro-replacement method. The purpose of their study was to verify the theoretical model proposed by Hughes and Withers (1974) [21] which are based on laboratory model tests. After the test, pile was excavated to check its deformed shape. The results of a site investigation supplemented by Cambridge and Menard pressuremeter tests were used to assess the limiting radial pressure. The results of the test prior to the field testing was predicted using theory given by Hughes and Withers (1974) [21] which is reviewed in Chapter 2. By assessing accurate pile diameter, the prediction of the load carrying capacity was excellent. This study demonstrated the importance of adopting correct soil and column properties. It was observed that deformed shape, shown in Figure 4.10, was similar to that observed by Hughes and Withers (1974) [21].

In this section, the load-settlement response of isolated granular pile given by Hughes et al. (1975) [22] are reproduced using FEM based software PLAXIS. As the field test was completed in duration of 30 minutes, it might be assumed that the soil deformed under undrained conditions. The same was modeled in PLAXIS by choosing the type of soil behavior as *undrained.* The granular pile material is considered as a purely frictional dilatant material, whereas the soft soil is taken to possess purely undrained shear strength. The site is uniform with 1-2 m thick layer of stiff clay underlain by soft clay to a depth of about 9 m. Medium dense sand is found underneath this layer. This layer may be considered as a stiff stratum. Depth of pile is considered as 9 m and the ground water table is located at 2 m below the surface. The initial column diameter of pile was estimated as 730 mm after excavating the granular pile from ground after testing. The basic soil parameters required for finite element analysis can be assessed from the available data of site investigations. The soil shear strength profile was measured using the Menard and Cambridge pressurementers, Dutchcone, Vane shear tests and conventional undrained triaxial tests.
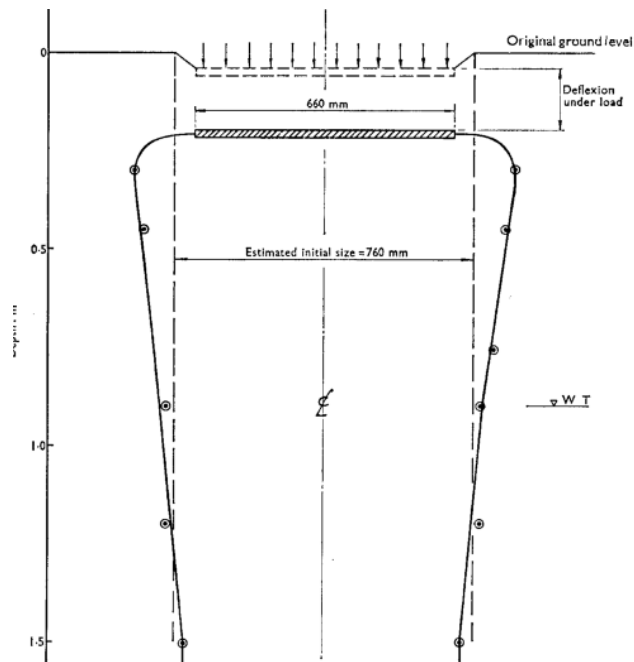
Figure 4.10: Deformed shape of granular pile after testing [22]

From the Cambridge pressuremeter tests, profile is taken as a relatively homogenous soil with an average cohesion of 22 kN/m^2. The cohesion profile of soil obtained from the conventional undrained triaxial testing on samples collected from the site and vane tests is shown in Figure 4.11. The same profile is used in finite elements analysis. The parameters of the GP and the soft clay used in PLAXIS are in this section are derived from Balaam (1978) [4] .
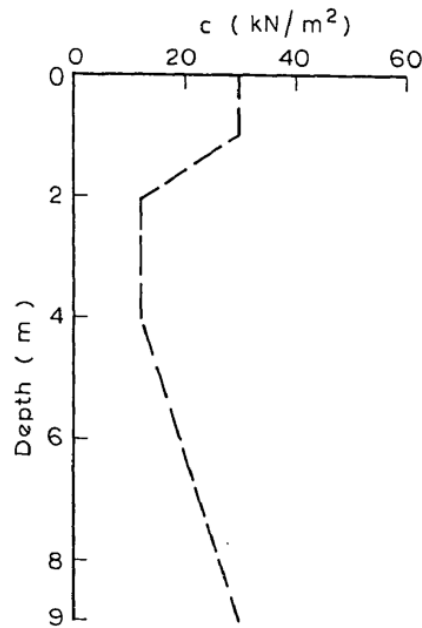
Figure 4.11: Strength profile of soil (Balaam 1978) [4]

To determine the deformation modulus of the clay, the radial stress-strain curves from the Cambridge pressuremeter is used. From this, an average value of 8000 kN/m^2 is adopted. A unit weight of 18 kN/m^3 is assumed for the both the pile and clay. Medium mesh is used for entire domain, and granular pile is further refined as shown in Figure 4.12.
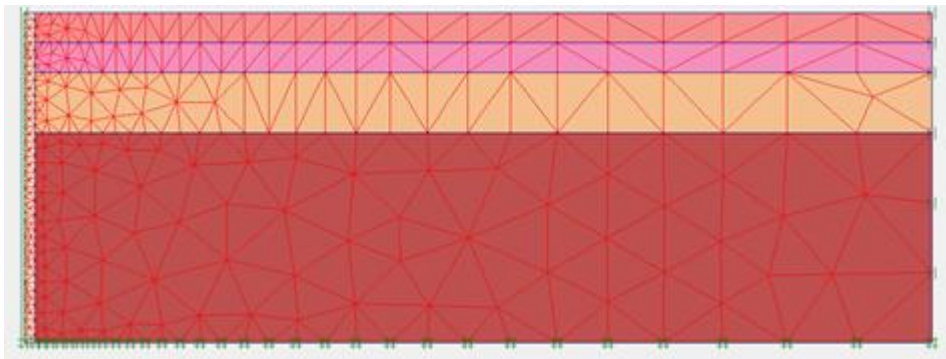

Figure 4.12: Mesh used for analysis of field plate load test

The friction angle and dilatancy angle are taken as 38° and 12°. The coefficient of earth pressure at rest K_0 is taken to be 1 in the pile region. The deformation modulus of granular pile which is back calculated from the elastic portion of the load-settlement curve and is taken as 50,000 kN/m^2. The load-settlement curve from PLAXIS, finite element analysis by Balaam (1978) [4] and field test by Hughes et al. (1974) [22] are compared here. The results from this study shows good agreement with Balaam's work and also shows reasonable agreement with field tests reported by Hughes et al. (1974) [22] as shown Figure 4.13.
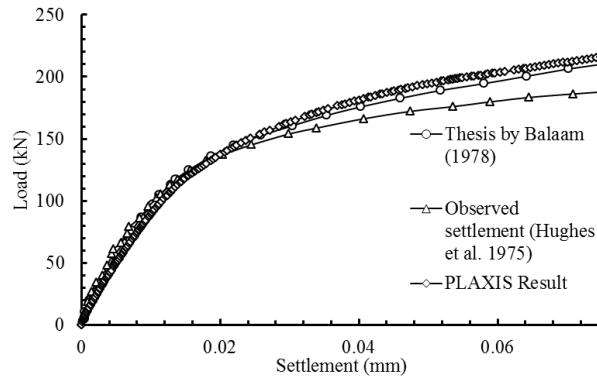
Figure 4.13: PLAXIS result compared with FE solution by Balaam (1978) [4] and load test by Hughes et al. (1975) [22]

4.4 Non-linear analysis of isolated floating granular pile

In order to analyse the single floating granular pile in semi-infinite mass of clay, it is modeled as axisymmetric case in software PLAXIS 2D v9. Since elastic response can only be applied for strains within elastic regime, elastic-perfectly plastic response of GP and clay are considered to model more realistic behavior. Granular pile of diameter 1 m and length 10 m is considered in the study. To study the effect of distance of boundary, both in lateral and vertical directions, distances are varied and the analysis is performed to obtain the load-settlement response (Figure 4.14). Based on the results, sizes of lateral and bottom boundaries are fixed as 35 times diameter of pile and 2 times the length of pile. In a similar fashion, mesh size is varied from coarse to very fine mesh. Medium and fine meshes were refined further for the whole domain with finest refinement within and near the GP. The load-settlement with various mesh configurations is shown Figure 4.15. The mesh configuration for which its effect on the load-settlement response is minimal should ideally be chosen for modeling. However, since fine mesh configuration will increase the computational effort, medium mesh for whole domain and refined mesh for GP area is considered. Further refinement mainly leads to more stress concentration in the area of granular pile.
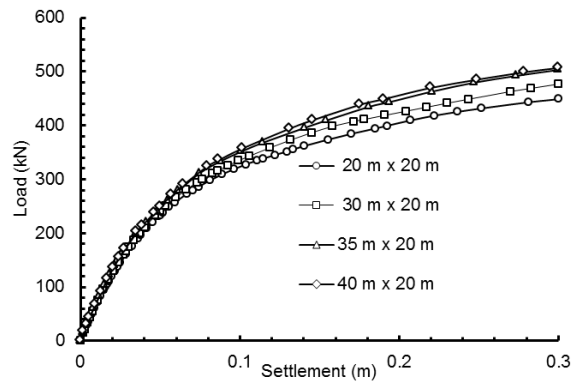
Figure 4.14: Effect of lateral and bottom boundaries on load-settlement behavior of GP
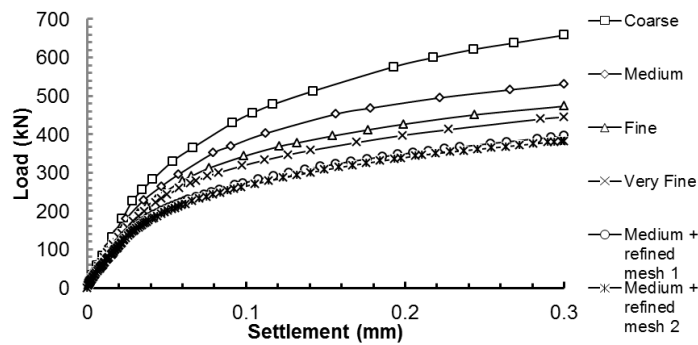

Figure 4.15: Effect of mesh configuration on load-settlement behavior of GP

Drained and undrained behavior are assumed for granular pile and clay, respectively. The input parameters (E, μ, c_u, φ, ψ, γ) are given in Table 4.4. To get equal vertical strain condition, load is applied as prescribed displacement of 30 cm. Water influence is not taken into account. 15-noded triangular elements are used because of its very accurate and high quality stress results. .

Table 4.4: Range of parameters of soft clay and Gp

Entity	Material Properties	Nominal Value	Range adopted
Soft clay	E_c (kN/m^2)	3750	2000-8000
	μ_c	0.5	-
	c_u (kN/m^2)	25	15-40
	γ_c (kN/m^3)	16	-
Granular Pile	E_p (kN/m^2)	37500	20000-50000
	μ_p	0.3	-
	c_{up} kN/m^2	0	0
	φ_p	38^0	30^0-50^0
	ψ_p	8^0	5^0- 15^0
	γ_p (kN/m^3)	20	-

The initial stress is simulated by using K_0 procedure. At the interface of granular pile, interface elements are not used since shear strength properties at interface between granular

pile and clay can vary depending on the method of installation. The model and deformed mesh is shown in Figure 4.16
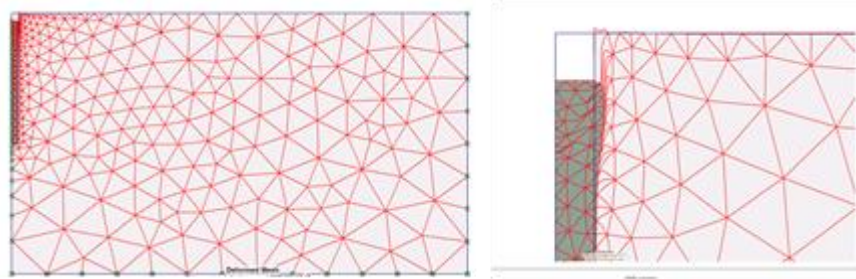

Figure 4.16: Finite element model and enlarged view of granular pile

In the following sections, bulging and load-settlement behavior of granular pile is described.

4.4.1 Bulging behavior of single floating granular pile

This study is focused on bulging behavior of single-isolated floating granular pile. To understand the bulging behavior of a GP, many studies based on numerical modeling, laboratory testing and field testing have been carried out. If the length of granular pile is greater than 4 to 6 times its diameter, the failure mechanism will be the bulging mode, irrespective of whether it is end bearing or floating pile [23]. The bulging failure is the most common failure criterion, since most of constructed GPs in the field have lengths equal to or greater than 4 to 6 times its diameter [15]. The lateral confinement from the surrounding soil influences the overall bulging behavior of the pile. Since the lateral confinement from the surrounding soil increases with the depth, bulging occurs near the surface and is suppressed away from the surface, except for cases such as the presence of intermediate layer of very weak soil like peat with thickness greater than about one pile diameter [6]. According to studies conducted by Barkdale and Bachus (1983) [6] and Nayak et al. (2010) [26], bulging depth will be equal to 2 to 3 times the pile diameter. Bulging depth is defined as the depth over which the lateral deformations of the granular material pile occur. Nayak et al. (2010) proposed that the maximum bulging occurs at a depth of 0.5 to 0.8 times the diameter of pile from surface [26]. Ambily and Gandhi (2007) reported that maximum bulging will occur at a depth of 0.5 times diameter of the granular pile, if the GP is loaded alone [3]. These studies consider the group effects of GPs using unit cell concept. Deb et al. (2011) observed that the maximum bulging occurs at a depth of 1.2 times of column diameter in the case of the granular pile embedded in clay and bulging diameter has a magnitude of 1.24 times the pile diameter[15]. Since these observations are based on small scale model tests, limitations of scale and boundary effects exist [15]. Field test findings on the bulging behavior of GP are also reported in the literature [8, 9, 21, 22]. In this study, the soil and GP parameters such as angle of shearing resistance and dilatancy angle of granular material, undrained

shear strength of soft clay, deformation moduli of granular material and soft clay, *etc.* are varied to study their influence on bulging behavior of GP. For this, finite element modeling was performed using PLAXIS 2D which is described in Chapter 3. As we discussed, bulging at top portion of granular pile can clearly be noticed as shown in Figure 4.14. This is mainly because of low confining stress developed near the top of the pile. In this parametric study, the effects of various properties of granular material and soft clay on the bulging depth, maximum bulging and the corresponding depth are studied. For the parametric study, values given as nominal value in Table 4.4 are used.

4.4.1.1 Effect of angle of shearing resistance of granular material

The influence of angle of shearing resistance of granular material, φ_p, on the bulging behavior is studied by varying φ_p from 30° and 50°. According to Brauns (1978) [12], bulging depth can be calculated using the equation

$$h = d. \tan(\pi/4 + \varphi_p/2) \tag{4.1}$$

where,

   h = Bulging depth

   d = diameter of GP

From this equation, it can be inferred that bulging depth will increase with increase in φ_p. Similar trend is noticed for granular pile modeled in the present study (Figure 4.17). Bulging depth varies from 3.75 m to 5.30 m with increase in φ_p. Maximum bulging is reduced from 20.7 mm to 10.61 mm as φ_p increases from 30° to 50°. This means that the tendency of bulging is reduced by increasing the angle of shearing resistance of granular pile. This is because as the angle of shearing resistance increases, shear resistance at the interface increases and hence, the lateral deformation of granular pile is reduced. Maximum bulging for various φ_p values occurs at a depth of 0.54 m to 0.97 m.
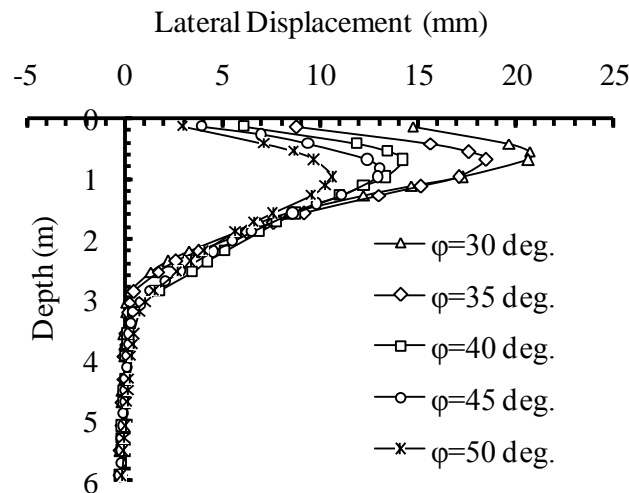
Figure 4.17: Influence of angle of shear resistance of granular pile on lateral displacements of GP

4.4.1.2 Effect of dilatancy angle of granular material

Figure 4.16 shows the bulging behavior for various dilatancy angles of granular material (ψ_p= 5° to 15°). The bulging depth is not affected by dilatancy angle of granular material. The maximum bulging increases from 14.8 mm to 18.4 mm as ψ_p increases from 5° to 15° (Figure 4.18). The depth at which the maximum bulging occurs varies from 0.827 m to 0.685m for ψ = 5° and ψ = 8°, respectively.

4.4.1.3 Effect of undrained shear strength of clay deposit

The influence of the undrained shear strength c_u of the surrounding clay on the performance of the granular pile is studied by varying c_u from 15 kPa to 40 kPa. As undrained shear strength increases, maximum bulging is found to decrease (Figure 4.19). This is because of its contribution towards the improvement of the column-soil interfacial shear resistance. Depth of maximum bulging ranges from 0.67 m to 0.76 m. The effect of c_u on the bulging depth is found to be insignificant.
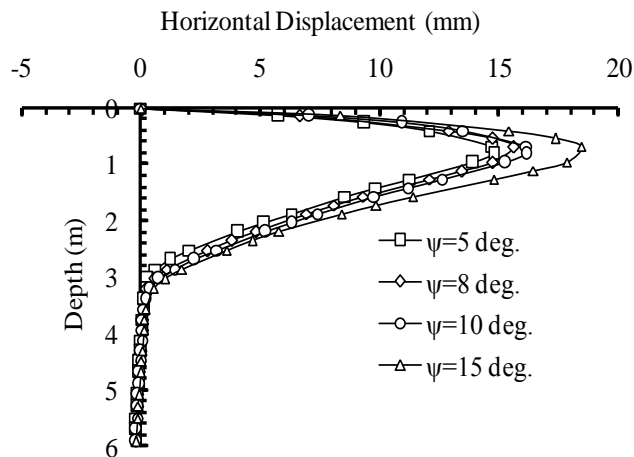
Figure 4.18: Influence of dilatancy angle of granular material on lateral displacements of GP
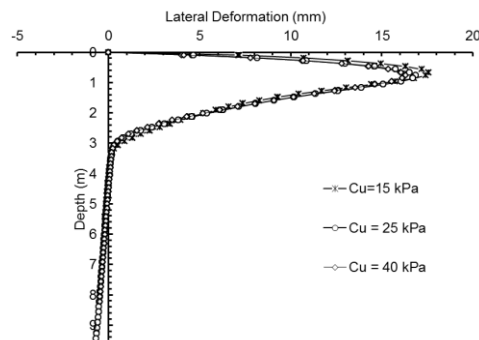

Figure 4.19: Influence of undrained shear strength of clay on lateral displacements of GP

4.4.1.4 Effect of loading

Instead of applying load, incremental prescribed displacement (up to 10 cm) is applied on the top of granular pile. Maximum bulging increases from 1.54 mm to 15.55 mm (Figure 4.20) corresponding to a prescribed vertical displacement of 1 cm and 10 cm, respectively. But, depth of maximum bulging is not affected by load increment. Bulging depth increases from 2.04 m to 4.31 m. Equation [Eq. (14.1)] proposed by Brauns (1978) does not consider the load effect on bulging depth. Zhang et al. (2012) [32] reported that values of maximum bulging increases with increase in load on the GP. Similar behavior of granular pile is observed in this study.
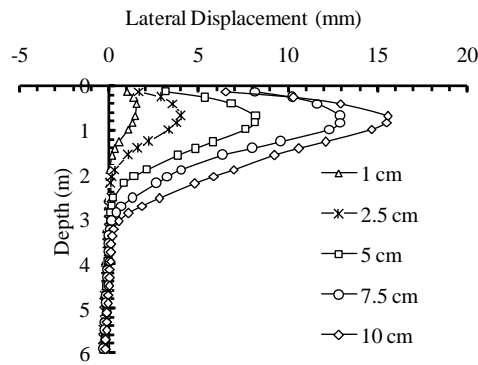
Figure 4.20: Lateral displacements for various prescribed displacement at the top of GP

4.4.1.5 Effect of deformation moduli of granular pile and clay

The influence of deformation modulus of granular pile, E_p, is studied for E_p=25,000 kPa to 50,000 kPa. The effect of E_p on the maximum bulging is found to be insignificant, the difference in the maximum bulging is found to be only 1 mm as E_p increase from 25,000 kPa to 50,000 kPa. The depth of maximum bulging and bulging depth is not affected by deformation modulus (Figure 4.21). To study the effect of deformation modulus of clay, E_c, is varied from 2500 kPa to 7500 kPa. The maximum bulging varies from 17.59 mm to 20.06 mm as E_c increases from 2500 kPa to 7500 kPa. But the effect of E_c on the depth of maximum bulging and bulging depth is found to be insignificant (Figure 4.22).
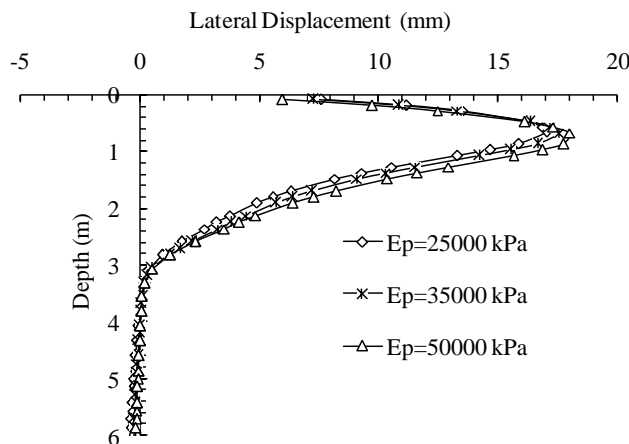

Figure 4.21: Influence of deformation modulus of granular pile on lateral displacements of GP

4.4.1.6 Effect of diameter of granular pile

The diameter of granular pile is varied from 40 cm to 100 cm to study its effect on the bulging behaviour of GP. The maximum bulging is not affected by variation of diameter of granular pile, as shown in Figure 4.23. But depth of maximum bulging and bulging depth are found to vary with the pile diameter. Bulging depth varies from 2.36 m to 4.2 m, whereas the depth at which maximum bulging occurs varies from 0.28 m to 0.67 m.

36

According to Braun's equation [Eq. (4.1)], bulging depth varies linearly with the diameter of granular pile. Similar behavior is observed in this study.
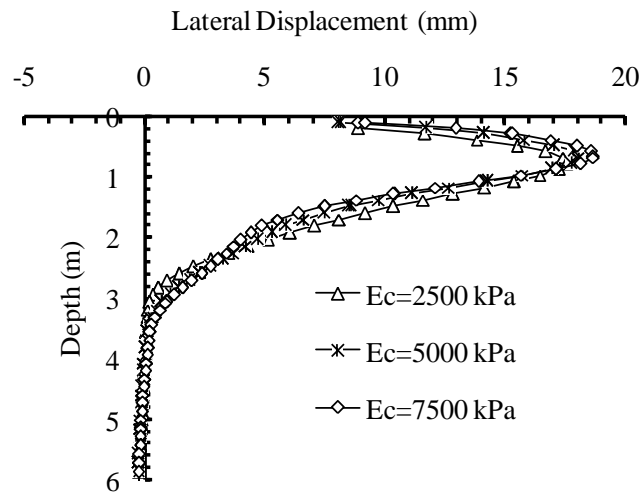
Lateral Displacement (mm)

Figure 4.22: Influence of deformation modulus of clay on lateral displacements of GP
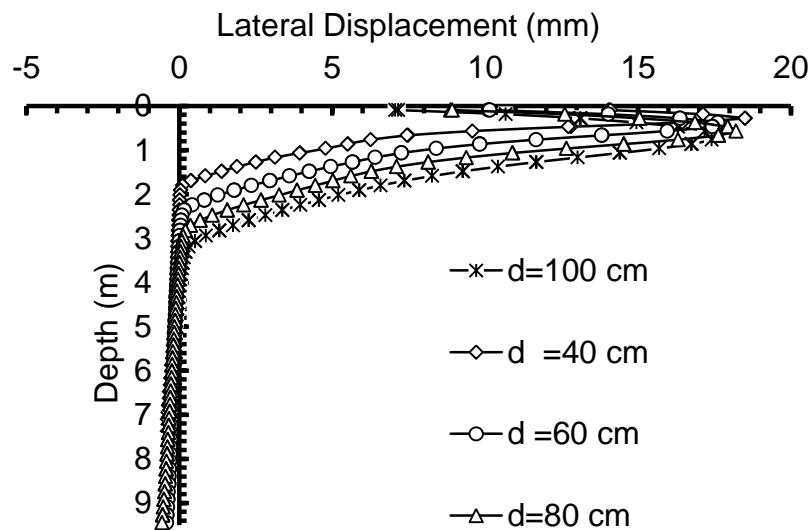
Lateral Displacement (mm)

Figure 4.23: Influence of diameter of granular pile on lateral displacements of GP

4.4.2 Load-settlement behavior of granular pile

In this section, the finite element analysis described in the previous Chapter 3 is used to determine the important GP and clay parameters that affect the load-settlement behavior of single floating GP. Range of parameters is tabulated in Table 4.4. Length and diameter of GP are taken as 10 m and 1 m, respectively. Same mesh configuration and boundary sizes are considered as given in the previous section. A prescribed displacement equal to 30% of pile diameter is applied at the top of GP for getting equal vertical strain. The finite element solutions show that considerable yield of both the granular material and the clay took place

while prescribed displacement is increased from 25 mm to 100 mm as shown in Figure 4.24.
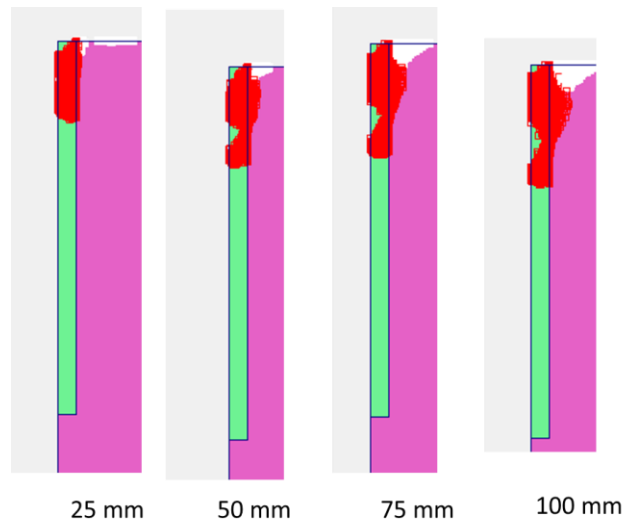

Figure 4.24: Growth of yielded zones in soil and GP

As the pile is formed by compacting different sizes of gravel, the mechanical properties of the GP will vary depending on the mechanical properties of material used and on the state of the material achieved. Numerical analysis is performed to assess the influence of angle of shearing resistance, dilatancy angle and stiffness (in terms of modular ratio) of GP on the load-settlement behavior of GP. The value of E_c/c_u and L/d is also varied to understand the effect of these parameters on load-settlement behavior. Normalized value of load (q^*) and settlement-diameter ratio (S/d), where S= settlement, is used for generating graphs.

$$q^* = Q/\pi d^2 c_u \tag{4.2}$$

where, Q is the applied load on the pile top

4.4.2.1 Influence of angle of shearing resistance of granular material

The influence of angle of shearing resistance of granular material, φ_p, on the load-settlement behavior is observed by varying φ_p from 30° to 50°. As φ_p is increased from 30° to 50°, the load carrying capacity of GP corresponding to a pile displacement of 10% of pile diameter is increased up to 41% (Figure 4.25). This is mainly due to increase in shear resistance offered by granular material with increase in φ_p. This leads to an increase in the load carrying capacity of GP as φ_p increases.
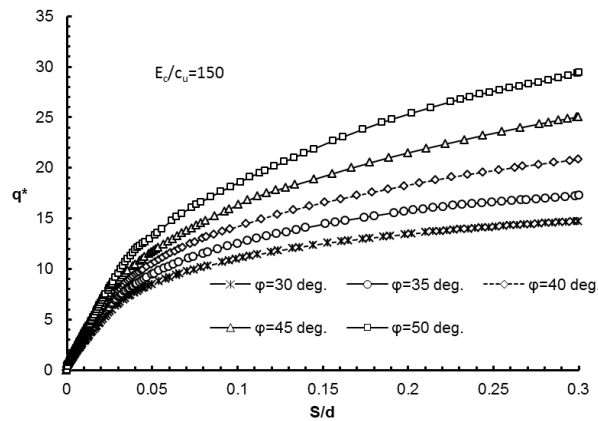
Figure 4.25: Influence of angle of shearing resistance of granular material on load-settlement behavior of GP

4.4.2.2 Influence of dilatancy angle of granular pile

Figure 4.26 shows the load-settlement behavior for various dilatancy angles of granular material ($\psi_p = 5^0$ to $\psi_p = 15^0$). The load carrying capacity increases up to 12.27 % for ψ_p increasing from 5^0 to 15^0. This may be due to an increase in the lateral confining stress for the case of a more dilatant material tending to increase in volume. The effect of dilatancy angle on the load-settlement behavior of GP is not significant in comparison to that of the effect of the angle of shearing resistance.
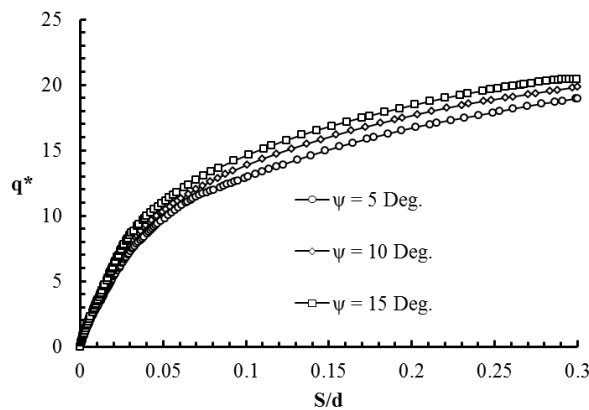

Figure 4.26: Influence of dilatancy angle of granular material on load-settlement behavior of GP

4.4.2.3 Influence of modular ratio

The stiffness of the granular material used for GP construction varies depending on the type of the material and the stiffness of the surrounding soil. To study effect of stiffness of GP, modular ratio (relative stiffness ratio) is considered. The range of modular ratio is varied from K=10 to K = 25 to observe its effect on load-settlement behavior of GP. For this range

39

of values, the influence of modular ratio on load-settlement behavior of GP is found to be insignificant (Figure 4.27).
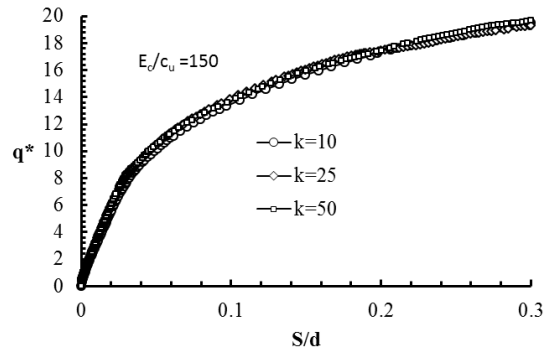

Figure 4.27: Influence of modular ratio on load-settlement behavior of GP

4.4.2.4 Effect of E_c/c_u ratio

Figure 4.28 shows the load-settlement behavior of granular pile for various value of E_c/c_u of clay. E_c/c_u value is varied from 100 to 200. As E_c/c_u increases from 100 to 200, load carrying capacity of GP increases up to about 21%. This is due to increase in confinement on GP with increase in E_c leading to larger load carrying capacity of GP for a given pile displacement.
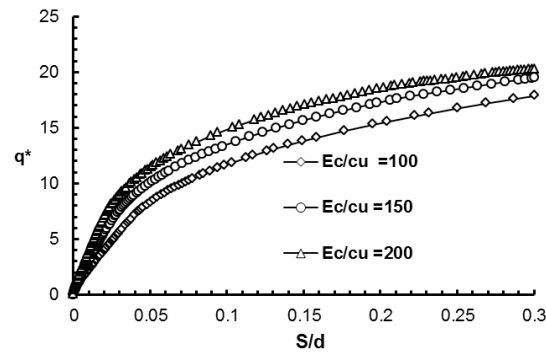

Figure 4.28: Influence of Ec/cu ratio on load-settlement behavior of GP

4.4.2.5 Influence of L/d ratio

In most cases, the length of the granular pile does not exceed 15 m. Length of GPs greater than about 10 m are usually not economically competitive with conventional deep foundations. Hence, range of L/d ratio is taken from 2 to 15. From this study, it can be observed that load carrying capacity of GP is increased for L/d = 2 to L/d = 3 as shown in Figure 4.29. After L/d = 3, there is no much increase in load carrying capacity indicating that a further increase in length of GP does not influence the load carrying capacity of GP.
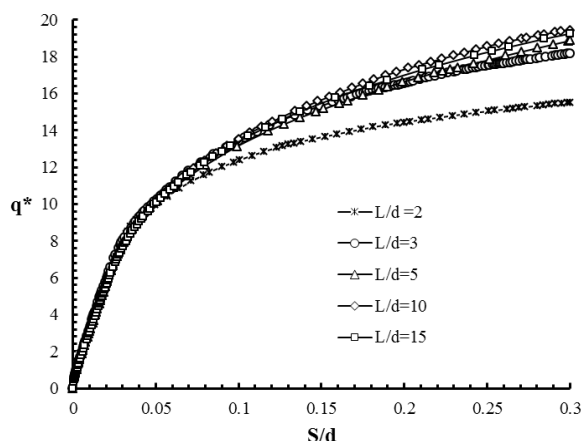
Figure 4.29: Influence of L/d ratio on load-settlement behavior of GP

4.4.3 Comparison of ultimate load carrying capacity of GP with existing theories

From the present study, the relationship between the angle of shear resistance of granular material, undrained shear strength of surrounding clay, and the ultimate vertical stress of isolated floating granular pile is compared with existing theories by Greenwood (1970) [20], Hughes and Withers (1974) [21], and Gibson and Anderson (1961) [19] (Figure 4.30). From PLAXIS analysis, the ultimate vertical stress of GP corresponding to 10 % and 20 % diameter of granular pile is used to compare with existing theories.
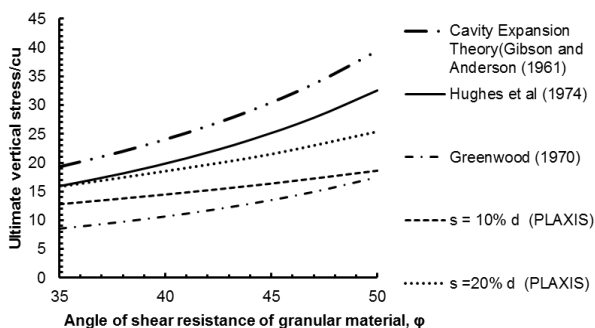

Figure 4.30: Comparison of ultimate vertical stress with existing theories

It can be observed that lower values are obtained from the method proposed in Greenwood (1970) [20]. This method obtains the ultimate load using the earth pressure theory treating the GP as a strip footing (plane strain condition) resting on a clay deposit. Hence, this method may not compare well with the ultimate load carrying capacity of GP obtained from the present study which is analysed by considering axisymmetry condition. From comparison of existing theories, it can be seen that higher values are obtained from Gibson and Anderson (1961) [19] which is based on cavity expansion theory by considering pure bulging mode of failure. PLAXIS result is more comparable with Hughes and Withers

41

(1974) [21]. Bergado and Lam (1987) [9] and Bergado et al (1984) [8] reported same range of ultimate load carrying capacity of GPs based on their experimental works.

4.5 Conclusions

The model is validated in finite element program software PLAXIS V9 with the linear stress-strain, and elastic- perfectly plastic analysis (including field test) of granular pile. The linear stress-strain analysis for granular pile compares well with Madhav et al. (2009). Elastic –perfectly plastic analysis of granular pile (unit cell concept) in PLAXIS shows good agreement with experimental result reported by Ambily and Gandhi (2007). The agreement between field test by Hughes et al. (1974), finite element solution by Balaam (1978) and PLAXIS result is found to be very good. The bulging and load-settlement behavior of single floating granular pile in semi-infinite medium of clay is studied. Angle of shearing resistance of the granular material, diameter of GP, and amount of load is found to have significant effect on the bulging behavior of GP. Brauns's equation is not appropriate to calculate the bulging depth since it does not consider the amount of load applied on the pile top. For a given value of d and E_c/c_u, well densified (higher value of φ_p) granular pile with high dilation angle acts stiffer and can take greater proportion of the applied load. Ultimate load obtained from PLAXIS 2D using Mohr-Coulomb model is found to compare well with Hughes et al. (1974). For a given value of d and E_c/c_u, the ultimate load of single pile corresponding to a displacement of 10% of the pile diameter is found to be proportional to the angle of shear resistance of granular material.

Chapter 5

Analysis of Isolated Floating Granular Piled Raft

5.1 Introduction

For relatively moderate loading from a structure, interest in the application of granular pile either single or in a small group is increasing in recent times. When the vertical load applied on the granular pile is increased, the lateral deformations or bulging of granular pile occurs. Bulging is more pronounced near to the surface due to low confining stresses near its top. Therefore, GPs typically fail from bulging as was observed from the findings reported from analysing of single floating granular pile (Chapter 4). Murugesan and Rajagopal (2010) [25] reported that strengthening the GP at the top portion can prevent bulging and consequently increase the load carrying capacity. It can be achieved by wrapping the individual granular piles with geosynthetics [25] or geogrid [17] or by encapsulating with a flexible sleeve/ horizontal disks [31] or by providing raft on the top of GP (GPR) [24]. Many research studies have been conducted on different methods, but the literature on the use of granular piled raft is limited. The available literature considers linear stress-strain response of soil and granular pile to study the effect of raft on the behavior of granular pile [24]. However, elastic response can only be applied for strains within elastic regime. In this study, elastic-perfectly plastic response of soil and GP are considered to model the behavior of granular piled raft.

5.2 Problem Definition

In this chapter, the load-settlement and bulging behavior of isolated granular piled raft in a semi-infinite medium of clay is studied. The objective of this study is to determine the important parameters affecting the behavior of GPR. In addition, critical length, bulging and load carrying capacity of GP and GPR is compared.
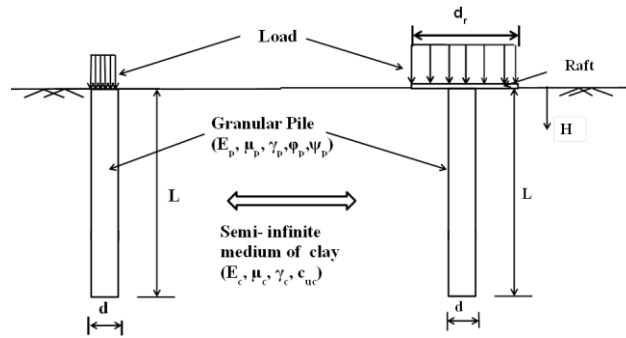
Figure 5.1: Schematic sketch of GP and GPR

5.3 Linear elastic analysis of granular piled raft (GPR)

As we did for the case of granular pile loaded alone (Chapter 4), granular pile is modeled with a length of 10 m and a diameter of 1 m. A rigid raft with a diameter of two times the diameter of GP is incorporated. Instead of providing the raft as a structural element in PLAXIS 2D, prescribed displacement is applied on the top of raft area (Figure 5.2). This models the raft as an infinitely rigid member. The soil is modeled as a single layer of clay with same properties as discussed in Chapter 4 (Table 4.1). Same boundary condition and mesh configuration are adopted for this model. The deformed mesh of granular piled raft and soil is shown in Figure 5.3. Different values of modular ratio K are considered for the analysis. The load taken by granular piled raft corresponding to 13 mm prescribed displacement is compared with solution by Madhav et al. (2009) [24]. The results from the present study show good agreement with Madhav et al. (2009) [24] as shown in Figure 5.4.
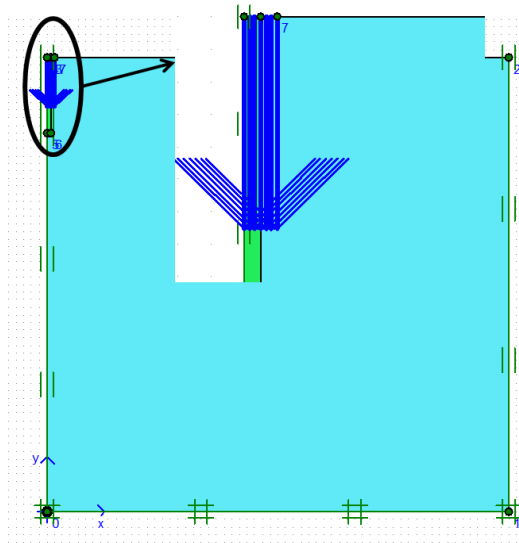
Figure 5.2: FE model granular piled raft with the insert showing an enlarged view near the pile top
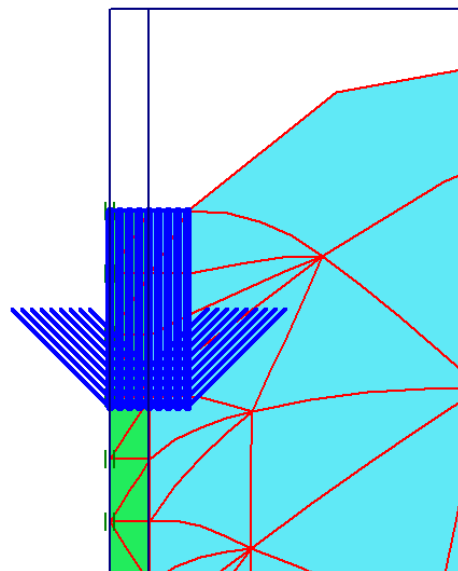

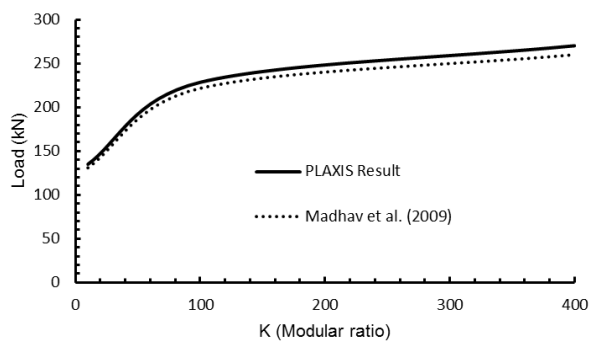**Figure 5.3: Deformed mesh of granular piled raft**

Figure 5.4: Comparison of results from present analysis with Madhav et al. (2009)

5.4 Non-linear analysis of granular piled raft

In this analysis, soft clay and granular pile is modelled using Mohr-Coulomb criterion (linear elastic-perfectly plastic) to simulate more realistic behavior. GPR is modelled as axisymmetric case. GP is of 10m in length and 1m in diameter. The convergence of results is carried out by changing the lateral and bottom boundaries and the mesh configuration. From the study, the size of lateral and bottom boundary is fixed as 35 times diameter of pile and 2 times the length of pile. For meshing, medium mesh is used for whole domain and further refinement is done for GPR area.
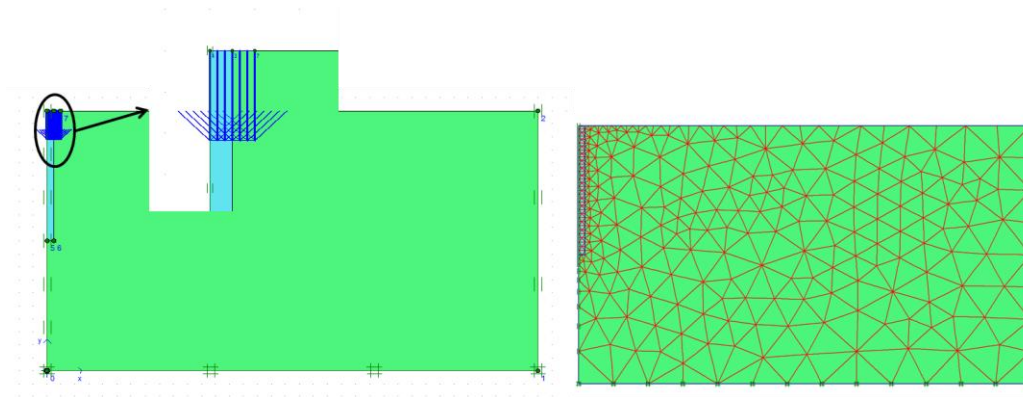

Figure 5.5: FE element model and mesh configuration of model

Drained and undrained behavior is assumed for granular pile and clay, respectively. The input parameters of GP and clay are given in Table 4.4. The effect of water table is not considered. Interface elements are not used in the analysis. In following sections, comparison between load-settlement behaviours of GP and GPR is studied.

5.5 Comparison between GP and GPR

5.5.1 Bulging behavior

To study the lateral deformation of granular piled raft, 10 cm prescribed displacement is applied on the raft. By comparing the deformed shape from the analyses performed on granular pile alone and granular piled raft (Figure 5.6), we can observe that lateral deformation is reduced and shifted from ground surface to some depth for GPR with respect to GP. Maximum bulging of GP is reduced from 16.1 mm to 11.2 mm (about 30 % reduction) when a raft is provided on top of GP. Depth of maximum bulging is shifted from 0.7 m to 1.32 m. Bulging depth is increased from 4.5 m to 5.5 m. Since load is applied over the full area of raft, the mean confining pressure on the GP is increased leading to less bulging. Lateral deformation of GP and GPR is shown in Figure 5.7.
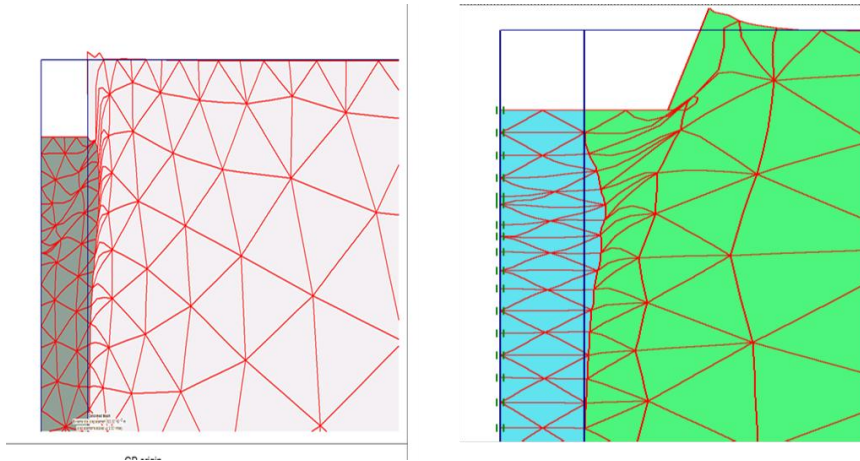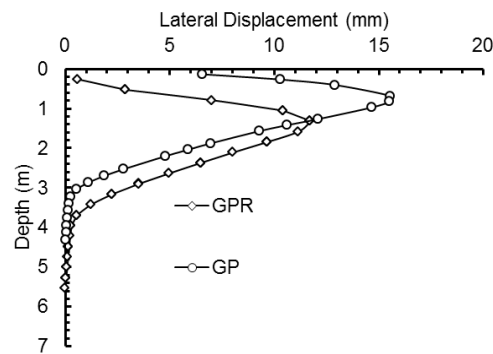
Figure 5.6: Deformed shape of GP and GPR

Figure 5.7: Comparison of lateral deformation of GP and GPR

5.5.2 Load-settlement behavior

In this section, load settlement behavior of granular pile and granular piled raft is compared. Prescribed displacement of 30 % of pile diameter is applied on the top of raft. Stress due to the applied load is shared by clay and granular pile. A portion of the load is transferred to the clay due to presence of raft and remaining portion of the load is taken by granular pile. Hence, ultimate load (corresponding to settlement=10% d) of GPR is increased up to 121% to that of GP as shown in Figure 5.9. When the prescribed displacement is increased from 25 mm to 100 mm, plastic zones are developed inside granular pile and these zones are found to grow into surrounding clay. Due to high stress concentration at the edge of raft, plastic zone is also developed near to the edges. For a large prescribed displacement equal to 100mm, the plastic points are found to reach the edge of raft. When prescribed displacement up to 100 mm is reached, plastic zone is developed fully as shown in Figure 5.8.
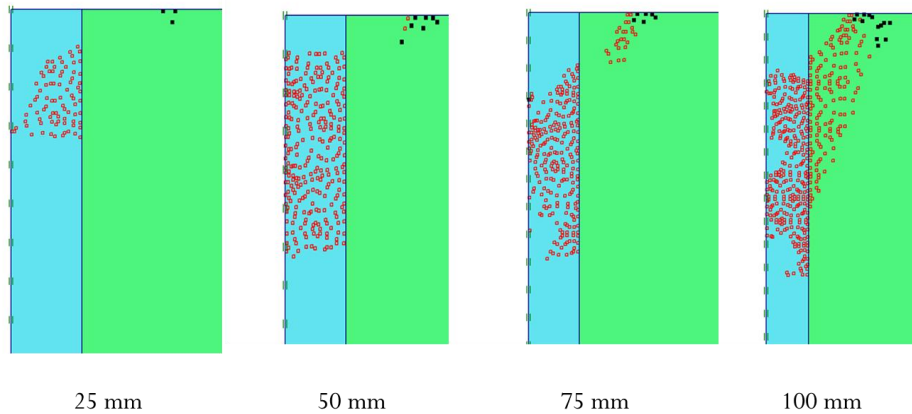
| 25 mm | 50 mm | 75 mm | 100 mm |

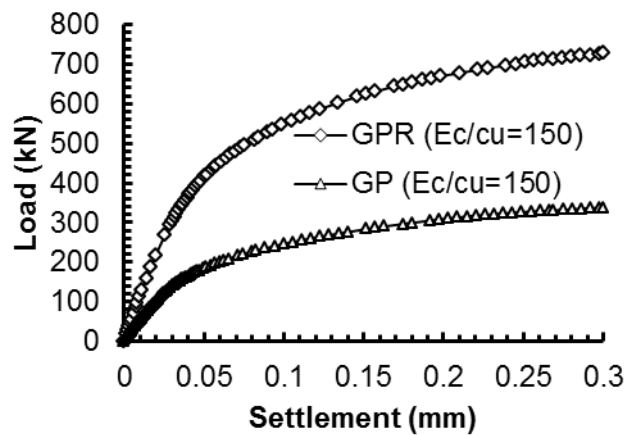**Figure 5.8: Growth of plastic zone with respect to loading**

Figure 5.9: Load carrying capacity of GP and GPR

5.5.3 Critical length

According to Hughes et al (1975), the critical length is defined as the minimum length at which both bulging and end bearing failure occur simultaneously. The basic assumption for critical length is that the clay/pile interface develops the full cohesion at failure. The critical length can be calculated by equating load corresponding to bulging failure and the sum of shaft friction resistance and end bearing force [22].

$$Q = c_u A_s + N_c c_u A_p \qquad\qquad (5.1)$$

where,

Q is the ultimate load carrying capacity

N_c is the appropriate bearing capacity factor which is taken as 9 for a long GP

A_s is the surface area $\pi d L_c$ of granular pile of diameter equal to d

L_c is critical length of granular pile

A_p is the cross-sectional area $\pi d^2/4$

48

In Figure 5.10, we can observe that plastic points are developed at the bottom of GP for L =2m. But there is no full development of plastic points at the bottom of GP for pile lengths L=3 m and 5 m. For granular pile with L =10 m, plastic points are only developed at the top portion of GP. This indicates that only bulging failure is governing the failure mode if length is greater than 3 m. Hence, critical length of GP will be in the range 2 m -to- 3 m for this case.
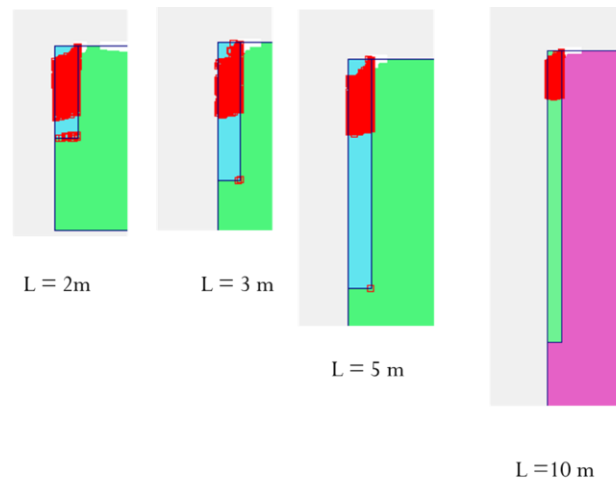

L = 2m   L = 3 m

L = 5 m

L =10 m

Figure 5.10: Development of plastic zone with respect to length of granular pile

Using cavity expansion theory [19] and Hughes and Withers (1974) [21] study, critical length of GP is calculated as 3.25 m and 2.29 m, respectively. If the length of granular is less than critical length, the governing failure criterion will be pile failure. Otherwise, it will be bulging mode of failure.

According to Vidyaranya et al. (2006) [30] if failure of granular pile is governed by bulging mode, the ultimate load carrying capacity of GP will be independent of L/d ratio as shown in Figure 5.11. A similar pattern of behavior is observed in the analysis of GP from the present analysis as shown in Figure 5.12. Beyond critical length of GP, there is no further improvement of load carrying capacity of GP.
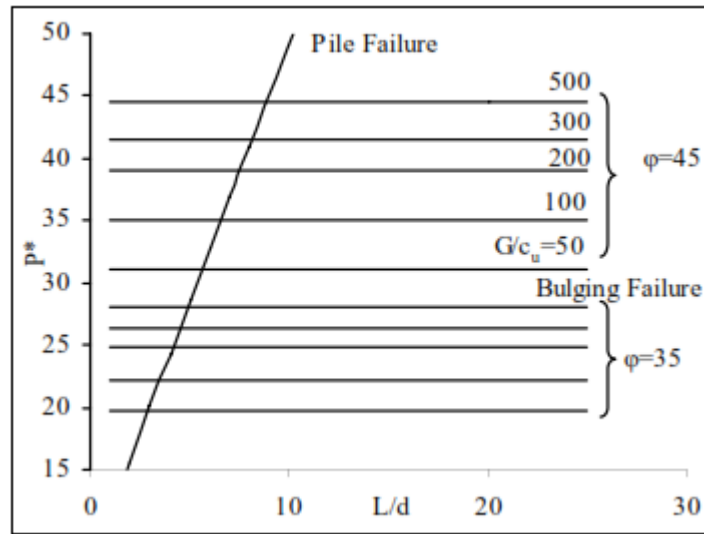
Figure 5.11: Variation of ultimate compressive load with L/d and G/Cu for different φ_p [30]
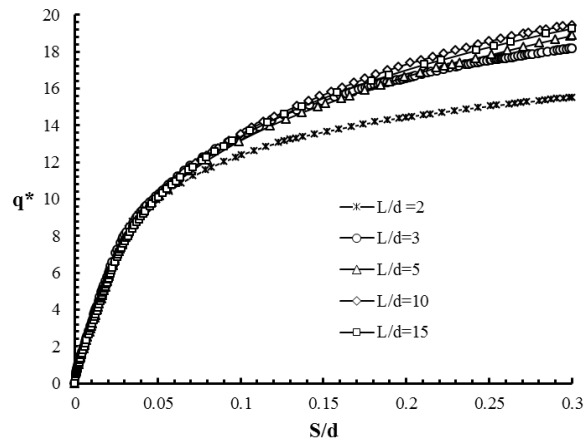

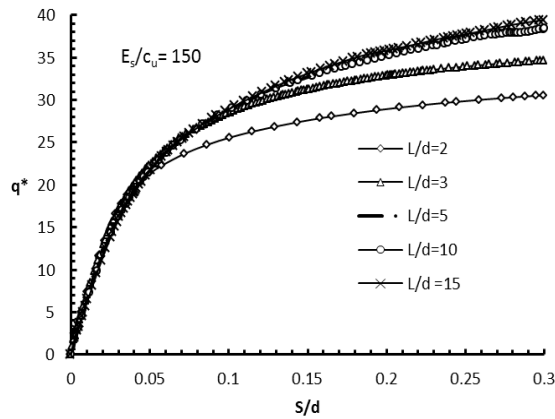**Figure 5.12: Effect of L/d ratio on load carrying capacity of GP**

Figure 5.13: Effect of L/d ratio on load carrying capacity of GPR

By providing the raft on the top of GP (GPR), critical length of granular pile can be increased. It can be proved by analysing load-settlement behavior of GPR for various L/d ratios as shown in Figure 5.13. Beyond L/d =5, there is no further improvement of the load carrying capacity of granular pile. It indicates that bulging is the governing failure mode of granular pile if L/d ratio is greater than/equal to 5. Hence, critical length will be in between 3 m and 5 m for a GPR of 1 m diameter.

5.6 Load settlement behavior of single floating granular piled raft

In this section, load-settlement behavior of granular piled raft is studied. To apply equal vertical strain, prescribed displacement equal to 30 % of pile diameter is applied on the top of raft. Range of parameters considered in the study is tabulated in Table 4.4. Numerical analysis is performed to assess the influence of angle of shear resistance and dilatancy angle of granular material, E_c/c_u ratio, L/d ratio and d/d_r ratio on load-settlement behavior of GPR. Length and diameter of GP is taken 10 m and 1 m, respectively. Normalized value of load q^* (Eq. 4.2) is plotted against S/d ratio, where S is the prescribed settlement at the top of the raft.

5.6.1 Influence of angle of shearing resistance of granular material

The influence of angle of shearing resistance, φ_p, on the load-settlement behavior is studied by varying its value from 30^0 to 50^0. As φ_p increases from 30^0 to 50^0, load carrying capacity of GP, corresponding to 10% of pile diameter, is increased up to about 29% as shown in Figure 5.14. This is due to more shearing resistance offered along the pile interface.
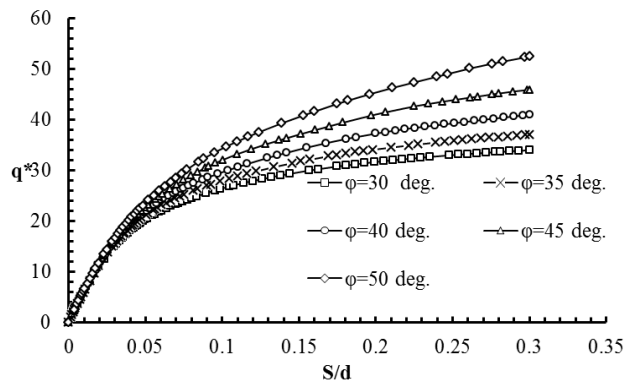
Figure 5.14: Influence of angle of shear resistance of granular material on load-settlement behavior of GPR

5.6.2 Influence of dilatancy angle of granular pile

Figure 5.15 shows the load-settlement behavior for various dilatancy angles of granular material ($\psi_p = 5^0$ to $\psi_p = 15^0$). For single granular pile, the load carrying capacity increases up to 12.27 % (Figure 4.26). For GPR, the effect of dilatancy angle on load carrying capacity of granular material is found to be insignificant. The confining stress on GP may be predominant leading to suppression of tendency to dilate.
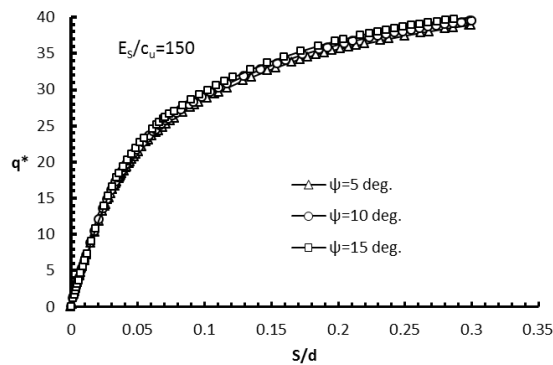
Figure 5.15: Influence of dilatancy angle on load-settlement behavior of GPR

5.6.3 Influence of E_c/c_u ratio of clay

Figure 5.16 shows the load-settlement behavior of granular piled raft for various values of E_c/c_u of clay. Its value is varied from 100 to 200. By increasing the value of E_c/c_u, load carrying capacity of GP increases up to about 21 % and 29 % for GP alone (Figure 4.28) and GPR, respectively. This is due to increase in confining stress on granular pile as E_c increases.
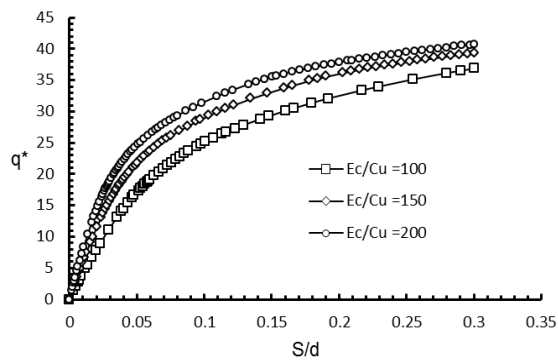
Figure 5.16: Influence of E_c/c_u ratio on load-settlement behavior of GPR

5.6.4 Influence of modular ratio

Modular ratio is varied from K =10 to 25 to observe its effect on load-settlement behavior of GP. For this range of values, it is found that there is no significant influence of modular ratio on load-settlement behavior of GPR as shown in Figure 5.17.
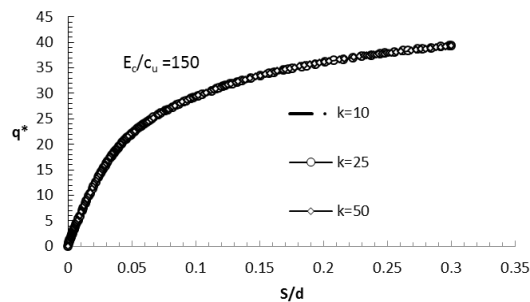
Figure 5.17: Influence of modular ratio on load-settlement behavior of GPR

5.6.5 Influence of d_r/d ratio of granular pile

To study the effect of d_r/d ratio on load-settlement behavior of GPR, the ratio is taken in the range 1.5 to 3. By increasing the d_r/d ratio, load carrying capacity of GPR increases as shown in Figure 5.18. This is due to increase in overburden pressure on granular pile as diameter of raft increases. Load taken by raft will increase and this will lead to more confinement to the pile.
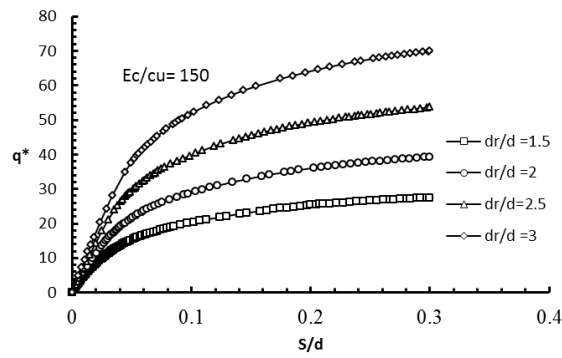
Figure 5.18: Effect of d_r/d ratio on load-settlement behavior of GPR

5.6.6 Influence of L/d ratio

Figure 5.19 shows the load-settlement behavior for various L/d ratio of granular piled raft (L/d =2 to L/d =15). The load carrying capacity of GPR increases as L/d increases. The increases in the load carrying capacity are not significant for L/d ratio greater than or equal to 5. This is because the bulging mode of failure governs the behavior of GPR as discussed earlier in Section 5.5.3.
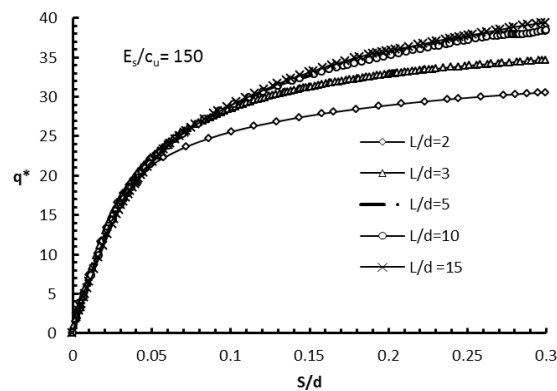
Figure 5.19: Effect of L/d ratio on load-settlement behavior of GPR

5.7 Conclusions

The proposed model used in finite element analysis using PLAXIS 2D v9 is validated for the linear stress-strain analysis of granular piled raft. The linear stress-strain analyses for granular piled raft compares well with Madhav et al. (2009). The load carrying capacity of GP is enhanced by providing raft on the top of granular pile. In this study, the ultimate load (corresponding to the settlement equal to 10% d) of GPR increases up to 121% compared to that of GP. Bulging of granular pile can be reduced with the provision of a raft. From this study, 30% reduction in bulging is observed for granular piled raft compared to that for the case of granular pile loaded alone. There is also increase in its critical length with the provision of the raft. If the length of GPR is greater than its critical length, bulging mode

governs the failure and ultimate load will not be affected by L/d ratio. Angle of shear resistance of granular material, d_r/d and E_c/c_u of clay are found to have significant influence on the load-settlement behavior of GPR for length of pile greater than or equal to critical length.

Chapter 6

Conclusions

In this study, behavior of single floating granular pile and piled raft embedded in a semi-infinite medium of clay deposit is analysed using finite element method with the help of the software package PLAXIS 2D. Among the possible failure mechanisms of the granular pile, bulging failure has been considered, since it is the common failure criterion of long granular pile. When load is applied in short time, clay will behave as a purely cohesive incompressible material whereas response of the pile material will be that of a purely frictional dilatant material. Finite element analyses have been carried out in which the following cases are taken into account to understand bulging and load-settlement behavior:

- o   Single floating granular pile (GP)
- o   Single floating granular piled raft (GPR)

6.1 Single floating granular pile

- The FE model in PLAXIS is validated by comparing the results from linear stress-strain analysis of granular pile with that of the results from Madhav et al. (2009) obtained by solving the elasticity solutions using finite difference method. The linear stress-strain analyses for granular pile compares well with Madhav et al. (2009).

- Non-linear analysis of granular pile (unit cell concept) in PLAXIS is compared with experimental and finite element analysis of pile group by Ambily and Gandhi (2007). Here, linear elastic-perfectly plastic response of GP and clay is taken into account to simulate more realistic behavior of both materials. The numerical results show good agreement with the results from experimental and finite element studies reported by Ambily and Gandhi (2007).

- Finite element analysis has also been used to reproduce the results of a previously published full scale plate load test by Hughes et al. (1975). The results from the

56

present finite element analysis are found to be in good agreement with the results reported by Hughes et al. (1974) and Balaam (1978). It is observed that the PLAXIS analysis is capable of predicting the response of a single floating granular pile, if the material properties and geometry of GP are well defined from field test. The bulging and load-settlement behavior of single floating granular pile in semi-infinite medium of clay is studied. It is observed that the long GPs will fail from bulging that takes place near the surface due to less confinement or lateral support. Angle of shearing resistance of the granular material, diameter of GP and amount of load applied on the pile top are found to have significant effect on the bulging behavior of GP. Brauns's equation is not appropriate to calculate the bulging depth as the equation does not account for the load applied on the top.

- The ultimate load carrying capacity of single floating granular pile is compared with available theories which are based on bulging mode of failure. Ultimate load obtained from PLAXIS 2D using Mohr-Coulomb model is found to compare well with empirical equation developed by Hughes et al. (1974) from experimental studies. For a given value of d and E_c/c_u, the ultimate load of single pile is proportional to the angle of shear resistance of granular material.

6.2 Single floating granular piled raft

The bulging and load-settlement behavior of single floating granular piled raft is studied by considering elastic-perfectly plastic behavior of both pile and clay.

- The model is validated in finite element program software PLAXIS 2D for the linear stress-strain analysis of granular piled raft. The linear stress-strain analysis for granular piled raft compares well with Madhav et al. (2009).

- Analysis of the granular piled raft, it is observed that the load carrying capacity of GP is enhanced with the provision of raft on the top of granular pile. In this study, ultimate load (corresponding to the settlement equal to 10 % diameter of GP) of GPR increases up to 121% compared to that of GP.

- Bulging of granular pile can be reduced with the provision of raft. In this study, 30 % reduction in bulging of granular piled raft compared to granular pile is observed.

The depth of maximum bulging and bulging depth shifts to a larger depth from the surface because of confinement effect of raft.

- The critical length of GP and GPR is compared. It can be observed that critical length of granular piled raft is increased. If the length of both GPR and GP is greater than its critical length, bulging mode will be the governing failure criterion and ultimate load will not be affected by L/d ratio.

- Load-settlement behavior of GPR is studied. For given value of d and E_c/c_u, angle of shearing resistance (φ_p) and d_r/d ratio of granular material are found to have significant influence on the load-settlement behavior of GPR with the length of pile greater than or equal to critical length.

Hence, for low-rise building founded on clay deposit, granular piled raft can be used as an efficient reinforcement method to enhance the load carrying capacity and prevent bulging, since single floating granular pile is not sufficient to reduce bulging due to less confinement near the top of granular pile.

References

[1]   H. Aboshi and N. Suemastu. The sand compaction pile method: State-of-The-Art-Paper. Proc. 3rd Int. Geotech. Seminar on Soil Improvement Methods, Nanyang Technological Institution, Singapore.

[2]   M. Alamgir, N. Miura, H. B. Poorooshasb, and M. R. Madhav. Deformation analysis of soft ground reinforced by columnar inclusions. Computers and Geotechnics 18 (4), (1996) 267-290.

[3]   A. P. Ambily and S. G. Gandhi. Behavior of stone columns based on experimental and FEM analysis. J. Geotechnical and Geoenvironmental Engineering ASCE 133(4), (2007) 405-415.

[4]   N. P. Balaam. Load-settlement behaviour of granular piles. Phd Thesis, The University of Sydney, June 1978.

[5]   N. P. Balaam and J. R Booker. Analysis of rigid rafts supported by granular piles. International Journal for Numerical and Analytical Methods in Geomechanics 5(4), (1981) 379-403.

[6]   R. D. Barkdale and R. C. Bachus. Design and construction of stone columns. FHWA/RD-83/026, Federal Highway Administration, Washington, D.C, (1983).

[7]   V. Baumann and G. E. A. Bauer. The performance of foundation on various soils stabilized by vibro-compaction method. Canadian Geotechnical Journal 11, (1974) 509-530.

[8]   D. T. Bergado, G. Rantucci and S. Widodo. Full scale load tests on granular piles and sand drains in the soft bangkok clay. Proc. Intl. Conf. on Insitu Soil and Rock Reinforcement, Paris, (1984) 111-118.

[9]   D. T. Bergado, and F. L. Lam. Full scale load tests on granular piles with different densities and different proportions of gravel and sand in the soft Bankok clay. Soils and Foundations 27(1), (1987) 86-93

[10] D. T. Bergado, J. C. Chai, M. C. Alfaro and A. S. Balasubramaniam. Improvement techniques of soft ground in subsiding and environment, A.A Balkerna Publishers, (1994)

[11] M. Boussida, B. Jellali and A. Porbaha. (2009). Limit analysis of rigid foundations on floating columns. International Journal of Geomechanics 9(3), (2009) 89-101

[12] J. Brauns. Die anfangstraglast von schottersäulen im bindigen untergrund. Die Bautechnik 55 (8), (1978) 263-271.

[13] R. B. J. Brinkgreve, W. Broere and D. Waterman. PLAXIS 2D- version 9.0, The Netherlands

[14] K. R. Datye and S. S. Nagaraju. Installation and testing of rammed stone columns. Proc. of IGS Specialty Sessions, 5th ARC on SMFE, Banglore, 101-104

[15] K. Deb, N. K. Samadhiya and J. B. Namdeo. Laboratory model studies on un reinforced and geogrid-reinforced sand bed over stone-column-improved soft clay, Geotextiles and Geomembranes, Technical Note, (2011) 190-196.

[16] J. M. Duncan and A. L. Buchignani. Engineering manual for settlement studies. Virginia Tech, Blacksburg, VA (1987)

[17] M. Elsawy, K. Lesny and W. Richwien (2010). Performance of geogrid- encased stone columns as a reinforcement. Numerical Methods in Geotechnical Engineering, Benz & Nordal (eds)© 2010 Taylor & Francis Group, London, ISBN, (2010) 875-880.

[18] K. Engelhardt and K. Kirsch. Soil improvements by deep vibratory techniques. Proc. 5th South-East Asian Conf. on Soil Engineering, Bankok, Thailand, (1977) 377-387.

[19] R. E. Gibson and W. F. Anderson (1961), In situ measurements of soil properties with the pressuremeter, Civil Engineering and Public Works Review 56(658).

[20] C. A. Greenwood. Mechanical improvement if soft soils below ground surface. Proc. Ground Engineering Conf., Inst. of Civil Engineers. London, June 11-12, 9-20.

[21] J. M. O. Hughes and N. J. Withers. Reinforcing of soft cohesive soils with stone columns, Ground Engineering, May, (1974) 42-49.

[22] J. M. O. Hughes, J. N. Withers and D. A. Greenwood. A field trial of the reinforced effect of stone column in soil. Geotechnique 25(1), (1975) 31-44.

[23] IS 15284 (Part 1), Design and construction for ground improvement- Guidelines Part 1 Stone columns. Bureau of Indian Standards, New Delhi, (2003).

[24] M. R. Madhav, J. K. Sharma and V. Sivakumar. Settlement of and load distribution in a granular piled raft. Geomechanics and Engineering 1(1), (2009) 97-112.

[25] S. Murugesan and K. Rajagopal. Studies on the behaviour of single and group of geosynthetic encased stone columns. J. Geotechnical and Geoenvironmental Engineering ASCE 136, (2010) 129-139.

[26] S. Nayak, R. Shivakumar and M.R.D. Babu. Performance of stone columns with circumferential nails, Ground Improvement, Proceedings of the Institution of Civil Engineers 164(G12), (2011) 97-106.

[27] R. Salgado . The Engineering of foundations, TaTa McGraw-Hill (2011)

[28] S. A. Tan, S. Tjahyono and K. K. Oo. Simplified plane –strain modelling of stone-column reinforced ground, J. Geotechnical and Geoenvironmental Engineering ASCE 134(2), (2008) 185-194.

[29] A. S. Vesic. Expansion of cavities in infinite soil masses. J. Soil Mechanics and Foundation Division ASCE 98(SM4), (1972) 265-290.

[30] B. Vidhyaranya, M. R. Madhav and S. R. Saibaba. Ultimate pullout capacity of granular pile anchors in homogenous ground. Geoindex, IGC 2006, 14-16 December (2006).

[31] C. S. Wu and Y. Hong. The behaviour of a laminated reinforced granular columns. Geotextiles and Geomembranes 26, (2008) 302-316.

[32] L. Zhang, M. Zhao, C. Shi and H. Zhao. Settlement calculation of composite foundation reinforced with stone columns, to appear in Intl. Jl. of Geomechanics, ASCE, (2012).